Ab initio investigation of the ground and low-lying states of the diatomic fluorides TiF, VF, CrF, and MnF

Constantine Koukounas, Stavros Kardahakis, and Aristides Mavridis[a)]
Laboratory of Physical Chemistry, Department of Chemistry, National and Kapodistrian University of Athens, P.O. Box 64 004, 15710 Zografou, Athens, Greece

(Received 5 February 2004; accepted 17 March 2004)

The electronic structure of the ground and low-lying states of the diatomic fluorides TiF, VF, CrF, and MnF was examined by multireference and coupled cluster methods in conjunction with extended basis sets. For a total of 34 states we report binding energies, spectroscopic constants, dipole moments, separation energies, and charge distributions. In addition, for all states we have constructed full potential curves. The suggested ground state binding energies of TiF($X\,^4\Phi$), VF($X\,^5\Pi$), CrF($X\,^6\Sigma^+$), and MnF($X\,^7\Sigma^+$) are 135, 130, 110, and 108 kcal/mol, respectively, with first excited states $A\,^4\Sigma^-$, $A\,^5\Delta$, $A\,^6\Pi$, and $a\,^5\Sigma^+$ about 2, 3, 23, and 19 kcal/mol higher. In essence all our numerical findings are in harmony with experimental results. For all molecules and states studied it is clear that the *in situ* metal atom (M) shows highly ionic character, therefore the binding is described realistically by M^+F^-. © *2004 American Institute of Physics.*
[DOI: 10.1063/1.1738412]

I. INTRODUCTION

We present *ab initio* calculations on the diatomic monofluorides MF, where M=first row transition metal element, Ti, V, Cr, and Mn. The inherent complexity of transition metal-containing molecules, makes the study of diatomics like MF ideal prototypes for the better understanding of larger molecular systems, as well as a reasonable testing ground for calibrating the capabilities and evolution of *ab initio* quantum mechanical methods. In addition, the comprehension of the chemical bond between a first row transition metal and a main group element is of considerable practical importance in the fields of organometallic chemistry, catalysis, high temperature chemistry, and even astrophysics.[1,2] It is known by now that spectra of diatomic molecules containing a $3d$ transition metal element are prominent in the spectra of cool stars and sunspots.[2] Although transition metal fluorides have not been observed in stars, the recent observation of AlF in the atmosphere of carbon stars,[2,3] suggests that fluoride diatomics such as MF could also be detected.

The reasons above, as well as our continuous interest in the electronic structure of transition metal-containing molecules, was the motivation for a systematic study of the MF, M=Ti, V, Cr, and Mn series.

Experimental interest on transition metal fluorides goes back to the mid-sixties, when Margrave and co-workers measured the dissociation energy (D_0) of ScF,[4] TiF,[5] CrF,[6] and MnF (Ref. 7) using high temperature mass spectrometric methods. The existing experimental literature on TiF, VF, CrF, and MnF is summarized in Table I. Note the conflicting experimental results on the identity of the TiF and VF ground states, and the lack of experimental D_0 values for the latter.

Practically all theoretical results on the MF series are listed in Table II. In 1987, Dement'ev and Simkin,[24] and in 1989, Averyanov and Khait[26] performed singles and doubles configuration interaction (CISD) calculations on TiF and VF, respectively. Recently, Boldyrev and Simons[25] studied the ground ($X\,^4\Phi$) and two excited states ($A\,^4\Sigma^-$,$^2\Delta$) of TiF using mainly coupled cluster singles and doubles with perturbative triples [UCCSD(T)] calculations, reporting dissociation energies, harmonic frequencies (ω_e) and dipole moments (μ). In 1999 Harrison[27] published an extensive multireference (MRCI) and coupled cluster [RCCSD(T)] study on CrF, including Darwin and mass-velocity relativistic corrections (Cowan–Griffin approach), dealing with the ground ($X\,^6\Sigma^+$) and six excited states, but he did not provide potential energy curves. We will contrast Harrison's results to our own in the Results and Discussion section. For reasons of completeness we would like to add at this point that 20 years ago Harrison published an extensive and insightful work on ScF, examining 30 states at the generalized valence bond (GVB)+CI/$[5s4p3d/_{Sc}3s3p1d/_F]$ *ansatz*.[28] Finally, Simard *et al.*,[17] reported experimental as well as *ab initio* MRCI results, studying theoretically the ground and seven excited states of CrF.

Presently, we report high level MRCI and RCCSD(T) (for the ground and first excited states) calculations using large to very large basis sets, for 8, 8, 7, and 11 states of TiF, VF, CrF, and MnF, respectively. To the best of our knowledge no theoretical calculations of any kind on MnF have been published heretofore. The TiF and VF excited states studied here span an energy range of about 1 eV, about 2 eV in CrF, and around 4.5 eV in the MnF case.

It is rather reasonable to assume that the bonding character of the MF molecules should have a dominant ionic component M^+F^- (see also Refs. 28 and 17). Therefore, and at least not far from the equilibrium geometry, we can envisage an M^+ metal cation interacting with the electric field created by the approaching F^- anion. This gives us a strong

a)Electronic mail: mavridis@chem.uoa.gr

TABLE I. Existing experimental data on TiF, VF, CrF, and MnF molecules. Dissociation energies D_0 (kcal/mol), bond distances r_e (Å), harmonic and anharmonic frequencies ω_e, $\omega_e x_e$ (cm^{-1}), rotational-vibrational constants α_e (cm^{-1}), and energy separations T_e (cm^{-1}).

Species	Ref./year	State	D_0	r_e	ω_e	$\omega_e x_e$	α_e	T_e
TiF	5/1967[a]		136 ±8					
	8/1969[b]	$X\,^4\Sigma^-$[c]			593			
	9/1985[d]	$X\,^2\Delta$[e]		1.832	678.4	2		
	2/1997[f]	$X\,^4\Phi$		1.8311	650.7[g]		0.0026	
		$G\,^4\Phi$		1.9192	532[g]		0.0022	
VF	10/1980[h]	$X\,^5\Pi$			571.4	3.8		
	11/2002[i]	$X\,^5\Delta$[j]		1.7758	670.4	2.7	0.0028	
		$?\,^5\Delta$		1.8769	557.4	1.5	0.0026	~10500
CrF	6/1965[k]	?	106.4±3.5					
	12/1991[l]	?	125 ±4.6					
	13/1995[m]	$X\,^6\Sigma^+$		1.7839	664.06	4.19	0.0031	
		$A\,^6\Sigma^+$		1.8916	581.4	1.97	0.0022	9953
	14/1995[n]	$B\,^6\Pi$			626[o]			
	15/1996[p]	$B\,^6\Pi$		1.8277	629.28		0.0027	8134
	16/1996[q]	$X\,^6\Sigma$		1.7876[r]				
	17/2001[s]	$D\,^6\Pi$						31700
MnF	7/1964[t]	?	101.2±3.5					
	18/1992[u]	$a\,^5\Sigma^+$		1.7854	645.92	3.22	0.0028	3000±1000[v]
		$c\,^5\Sigma^+$		1.8193	597.38	3.15	0.0031	14493[w]
	19/1992[x]	$d\,^5\Pi$		1.8137 (r_0)	640.0	3.6		19806[y]
	20/1993[z]	$X\,^7\Sigma^+$		1.8387	624.2	3.2[aa]		
		$A\,^7\Pi$		1.7923	648.0	1.6	0.0029	28526
		$d\,^5\Pi$		1.8101[bb]				19807
		$e\,^5\Sigma^+$						20220[cc]
	21/1994[dd]	$b\,^5\Pi_i$		1.7883	630.54	3.564	0.0024	11751[ee]
	22/1996[ff]		104.5±2.3					2500±500[gg]
	23/2002[hh]		106.4±1.8					

[a]Mass spectrometric study at high temperature.
[b]Electronic absorption spectroscopy.
[c]Assumed that $^4\Sigma^-$ is the ground state.
[d]Rotational analysis.
[e]Assumed that $^2\Delta$ is the ground state.
[f]Laser Fourier transform emission spectroscopy; that the *X*-state is of $^4\Phi$ symmetry is based on unpublished MCSCF results of J. F. Harrison.
[g]$\Delta G_{1/2} = \omega_e - 2\omega_e x_e$.
[h]Vibrational emission spectroscopy.
[i]Infrared emission spectroscopy.
[j]Although the authors suggest that the ground state of VF is $^5\Delta$, they do not rule out the $^5\Pi$ state.
[k]Mass spectrometry at high temperature.
[l]O. V. Boltalina, A. Y. Borshchevskii, and L. N. Sidorov, Russ. J. Phys. Chem. **65**, 466 (1991).
[m]Rotational spectroscopy.
[n]Rotational spectroscopy.
[o]$\Delta G_{1/2}$.
[p]Rotational spectroscopy.
[q]Rotational spectroscopy.
[r]$B_0 = 11369.61615$ MHz.
[s]Laser induced fluorescence spectroscopy.
[t]Mass spectrometry at high temperature.
[u]Rotational spectroscopy.
[v]$a\,^5\Sigma^+ - X\,^7\Sigma^+$ (or 3500±1000, Ref. 20).
[w]$c\,^5\Sigma^+ - a\,^5\Sigma^+$.
[x]Rotational spectroscopy.
[y]$d\,^5\Pi - a\,^5\Sigma^+$.
[z]Rotational spectroscopy.
[aa]Assumed.
[bb]Estimated from $r_0 (= 1.8137$ Å), assuming that $\alpha_e = 0.003\ cm^{-1}$.
[cc]$e\,^5\Sigma^+ - a\,^5\Sigma^+$.
[dd]Rotational spectroscopy.
[ee]$b\,^5\Pi_i - a\,^5\Sigma^+$.
[ff]Chemiluminescence emission spectroscopy.
[gg]$a\,^5\Sigma^+ - X\,^7\Sigma^+$.
[hh]High temperature mass spectroscopy.

clue on the manifold of low-lying states that one can expect. For instance, the ground $a\,^4\mathrm{F}(3d^2 4s^1)$ and second excited $a\,^2\mathrm{F}(3d^2 4s^1)$ states of Ti^+,[29] give rise to quartets and doublets of Σ, Π, Δ, and Φ symmetries, respectively, in an axial electric field. Similarly, in the V^+ case the ground state is $^5D(3d^4)$;[29] however its first and second excited states $a\,^5F(3d^3 4s^1)$ and $a\,^3F(3d^3 4s^1)$ 0.342 and 1.104 eV above the $a\,^5D$ and better disposed for bonding in the VF system, dictate low-lying Σ, Π, Δ, and Φ molecular states, quintets and/or triplets. Following the same line of thought, we con-

TABLE II. Published *ab initio* results on TiF, VF, CrF, and MnF.

Ref./year	State	r_e (Å)	ω_e (cm^{-1})	μ(D)[a]	T_e (cm^{-1})
		TiF			
24/1987[b]	$X\,^4\Phi$	1.832[c]			0.0
	$A\,^4\Sigma^-$				1452
1/1995[d]					807[e]
25/1998[f]	$X\,^4\Phi$	1.869	634	2.958[g]	0.0
	$A\,^4\Sigma^-$	1.832	638	3.110[g]	645
	$^2\Delta_r$	1.777	677	1.863[g]	2145
		VF			
26/1989[h]	$X\,^5\Delta$	1.871	621		0.0
	$^5\Pi(1)$	1.856	616		1700
		CrF			
27/1999[i]	$X\,^6\Sigma^+$	1.788	697	4.21[j]	0.0
	$^6\Pi$	1.838	633	2.36[j]	6135
	$^6\Delta$	1.882	600	2.81[j]	10133
	$A\,^6\Sigma^+$	1.919	554	4.36[k]	10373
	$^4\Sigma^+$	1.789	690	2.65[k]	8494
	$^4\Pi$	1.795	644	2.32[k]	11418
	$^4\Delta$	1.825	610	3.19[k]	15236
17/2001[l]	$D\,^6\Pi$	1.773	695		31900

[a]Dipole moment.
[b]Calculation of 17 states at the CISD/$[4s3p2d/_{Ti}2s1p1d/_F]$ level using Slater-type orbitals.
[c]Experimental value, the same for all states, from Ref. 3.
[d]As reported in Ref. 1; MCSCF approach.
[e]$A\,^4\Sigma^- - X\,^4\Phi$.
[f]UCCSD(T)/6-311++G(2*d*,2*f*); $1s^2$(F) and $1s^22s^22p^63s^23p^6$(Ti) e^- frozen; $D_e(X\,^4\Phi)=123.6$ kcal/mol.
[g]Calculated at the QCISD/6-311++G(*d*,*f*) level.
[h]Seventeen quintet states have been calculated at the multireference-CISD/$[7s4p2d/_V4s3p1d/_F]$ level and at a fixed $r=1.85$ Å. With the exception of $X\,^5\Delta$ and $^5\Pi(1)$ states only the T_e values are reported; $\omega_e x_e = 3.4(X\,^5\Delta)$, $2.6(^5\Pi)$ cm^{-1}.
[i]MRCI including the Cr($3s^23p^6$) core electrons in the CI procedure (=C-MRCI)+Darwin and mass-velocity relativistic corrections using a $[8s8p6d4f2g/_{Cr}6s5p4d3f/_F]$ basis. $D_e(X\,^6\Sigma^+)=107.7$ kcal/mol obtained indirectly through a RCCSD(T) calculation at equilibrium, the $Cr^+(^6S)$ and $F^-(^1S)$ RCCSD(T) energies, and the experimental ionization energies of Cr and F.
[j]C-MRCI//RCCSD(T)+relativistic corrections.
[k]C-MRCI//C-MRCI+relativistic corrections+Q (Q=Davidson correction).
[l]MRCI/[ANO-S/$_{Cr}5s4p3d2f/_F$].

sidered quartets and sextets of Σ, Π, and Δ, and quintets and septets of Σ, Π, Δ, Φ, and Γ symmetries for the CrF and MnF, respectively.

We believe that the present study will help experimentalists and theoreticians alike to better characterize and clarify the electronic structure of these chemically simple but otherwise fairly complex molecules.

II. BASIS SETS AND METHODS

For the fluorine atom the correlation consistent basis set of quadruple-Z quality augmented with a series of diffuse functions (aug-cc-pVQZ=AQZ), $13s7p4d3f2g$ was used, generally contracted to $[6s5p4d3f2g]$.[30] For the metal atoms the atomic natural orbital (ANO) Gaussian basis sets $21s16p9d6f4g$ (Ti) and $20s15p10d6f4g$ (V,Cr,Mn) were employed, similarly contracted to $[7s6p4d3f2g]$.[31] This one-electron space contains 164 spherical Gaussian functions and was used uniformly for the construction of all MF (M =Ti,V,Cr,Mn) potential energy curves (PEC) and for all states studied. In addition, and for all states of TiF and VF and for two states of CrF and MnF (ground and first excited), the effect of one additional h ($l=5$, $\alpha=0.8$) function was also examined. In addition, the newly developed Ti correlation consistent-type basis set(s) of Bauschlicher,[32] $21s16p9d$ contracted to $[7s8p6d]$ and augmented by a series of "polarization" sets, namely $2f1g$ (TZ), $3f2g1h$ (QZ), and $4f3g2h1i$ (5Z) were tested on the ground and first excited state of the TiF molecule. The corresponding basis sets for F were Dunning's aug-cc-pV*n*Z, $n=$T, Q, and 5 respectively.[30] Finally, in the core-correlated calculations of the TiF system (*vide infra*), in conjuction with the correlation consistent-type TZ, QZ, and 5Z basis, the latter were augmented by $1f$ (CTZ), $1f1g$ (CQZ), and $1f1g1h$ (C5Z) core-Gaussians.[32] Thus our largest contracted basis set used in the TiF molecule, $[7s8p6d5f4g3h1i/_{Ti}7s6p5d4f3g2h/_F]$, numbers 305 spherical Gaussians.

The complete active space self consistent field+single +double replacements (CASSCF+1+2=MRCI) method was employed to construct potential energy curves (PEC) for all four MF species and states. Although the MRCI approach is the most general and conceptually satisfying technique to understand bond formation—bond breaking problems it becomes computationally very demanding and complex as the number of active electrons increases, say, beyond 10. In the present case the number of valence electrons ranges from 11 (TiF) to 14 (MnF). However, by "chemical intuition," the $2s^22p_x^22p_y^2$ space of the F atom can be excluded from the active space with impunity. Thereby, our functional valence space chosen for the MF molecules is composed of 8 orbital functions, correlating asymptotically to the limited valence spaces of M($4s+3d+4p_z$) and F($2p_z$) atoms. Trial CASSCF calculations showed that the $4p_z$ function on the metal atoms are necessary for proper dissociation. Considering now the $1s^22s^22p^63s^23p^6$ and $1s^2$ electrons of M and F, as core (inactive), our zeroth-order spaces are formed by alloting 5, 6, 7, and 8 e^- among 8 orbitals, giving rise to 135, 110, 63, and 27 configuration functions (CF) for the TiF, VF, CrF, and MnF ground states, respectively. For the $A\,^7\Pi$ state of MnF only, and for reasons that will become clear later, the active space of the Mn atom was extended to $4s+3d+4p$, i.e., the total functional valence space comprises 10 orbitals instead of 8. It should be stated at this point that all our CASSCF wave functions obey symmetry and equivalence restrictions.

Dynamic valence correlation was extracted through single and double excitations out of the zero-order space(s) within the internal contraction (ic) *ansatz*[33] as implemented in the MOLPRO (Ref. 34) package. Our largest uncontracted CI expansion (VF, states $^3\Phi$ and $^3\Pi$) contains 73×10^6 CFs, reduced to about 2.4×10^6 internally contracted using the $[7s6p4d3f2g/_VAQZ/_F]$ basis. To estimate core ($3s^23p^6$) correlation effects with the above basis, ic-MRCI calculations were performed out of the CASSCF space(s) but including the $3s^23p^6e^-$ of the metal atoms in the CI process. These calculations will be referred to as C-MRCI. The number of CFs involved in the C-MRCI (ic C-MRCI) computations ranges from 137×10^6 (5.7×10^6) in the $X\,^4\Phi$ state of TiF, to 385×10^6 (9.3×10^6) in the $^4\Pi$ state of the CrF mol-

ecule. Using the correlation consistent-type basis set for the Ti atom,[32] the C-MRCI (ic C-MRCI) expansion in the $X\,^4\Phi$ state of the TiF system and for the largest basis set used ($[C5Z/_{Ti}A5Z/_F]$), consists of 532×10^6 (14.3×10^6) CFs.

For the TiF $X\,^4\Phi$ state we also report complete basis set (CBS) limits of r_e and D_e values, obtained by applying the mixed Gaussian/exponential relation $P_n=P_\infty+Ae^{-(n-1)}+Be^{-(n-1)^2}$, where P is a generic property, P_∞ its CBS-limit, n the cardinal basis set number, and A, B freely adjustable parameters.[35]

For reasons of comparison and at the $[7s6p4d3f2g/_M AQZ/_F]$ basis, valence restricted coupled-cluster singles and doubles including noniterative triples {RCCSD(T)} calculations were performed around equilibrium for all four MF molecules (M=Ti, V, Cr, and Mn) ground and first excited states. RCCSD(T) calculations including the $3s^23p^6$ core electrons of M will be referred to as C-RCCSD(T).

Scalar relativistic effects for all MF molecules and for the ground and first excited states were estimated at the (valence) MRCI level via the one-electron first order Douglas–Kroll (DK) approximation,[36,37] uncontracting at the same time the ANO and AQZ basis sets of the M and F atoms. Similar relativistic calculations and for the same states were performed at the C-MRCI level of theory. For the TiF $X\,^4\Phi$ and $A\,^4\Sigma^-$ states, DK calculations were done as described above, but using the uncontracted $C5Z/_{Ti}A5Z/_F$ correlation consistent-type basis set of the Ti atom.[32] The C-MRCI (uncontracted basis) expansion of the TiF $X\,^4\Phi$ state contains 830×10^6 CFs, reduced to 14.8×10^6 in the internal contraction scheme.

Size nonextensivity errors at the {MRCI,C-MRCI}/$[7s6p4d3f2g/_M AQZ/_F]$ (+Davidson correction=+Q) level for the TiF, VF, CrF, and MnF ground states are (in mhartrees), {12(4.5),34(12)}, {12(5.5),26(7.7)}, {13(3.4),29(7.8)}, and {14(5.4),28(8)}, respectively. On the average, a size nonextensivity error of 13(5) mh is observed at the MRCI (+Q) level of theory. Obviously, size nonextensive effects are the most deleterious drawbacks of the MRCI approach as the number of active electrons increases, particularly if one is interested in obtaining accurate dissociation energies. The situation is significantly ameliorated by using the supermolecule approach in calculating D_e values due to cancellation of errors and/or using the Davidson correction (+Q), or the multireference averaged coupled pair functional (MR-ACPF) approach of Gdanitz and Ahlrichs.[38] For this reason and in order to monitor our MRCI/$[7s6p4d3f2g/_M AQZ/_F]$ results, we also performed MR-ACPF calculations around equilibrium geometries for almost all states of the MF series. For the TiF, VF, CrF, and MnF ground states for instance, size nonextensivity errors at the MR-ACPF level are 2.0, 1.6, 0.3, and 0.7 mh, respectively, a significant improvement over previous results.

Two more things should be addressed: (a) Indicative basis set superposition error (BSSE) corrections were obtained by applying the usual counterpoise approach[39] in the ground states of the MF series at the MRCI/$[ANO/_M AQZ/_F]$ level. Our findings, 0.25, 0.29, 0.29, and 0.38 kcal/mol for the TiF, VF, CrF, and MnF X-states, respectively, suggest that BSSE-corrections are indeed small as compared to all other approximations and/or ommissions. (b) The state-average (SA) technique was used for most of the states of the MF series; namely all states of TiF and VF were pair-state-averaged as follows: $[^{4,2}\Phi,^{4,2}\Pi]$, $[^{4,2}\Sigma^-,^{4,2}\Delta]$ for TiF, and the corresponding triplets and quintets for VF. For CrF only two states were state-averaged, i.e., $[X\,^6\Sigma^+,A\,^6\Sigma^+]$, while for MnF 8 out of the 11 calculated states were state-averaged in groups of 3 and 5, i.e., $[b\,^5\Delta,d\,^5\Sigma^+,f\,^5\Gamma]$, and $[c\,^5\Pi, e\,^5\Phi,g\,^5\Pi,h\,^5\Pi,i\,^5\Pi]$.

Finally, spectroscopic constants (r_e, ω_e, $\omega_e x_e$, and α_e) were determined through a Dunham analysis, while dipole moments (μ) at the MRCI, C-MRCI level were obtained as expectation values ($\langle\mu\rangle$), and also through the finite field method (μ_{FF}).

III. ATOMIC STATES OF Ti, V, Cr, AND Mn

Table III lists total energies and ionization potentials (IP) of the Ti, V, Cr, and Mn series in a variety of methods at the ANO-$[7s6p4d3f2g]$ basis. We examine the IPs of the M atoms because in the M–F series and in all states examined, the *in situ* M is highly ionized (see below). Contrasting experimental vs theoretical IPs, we first observe that the MRCI (+Q) numbers are in fair agreement with experiment, the differences being ΔE(expt−theory)=0.170(0.159), 0.356 (0.243), 0.366 (0.316), and 0.338 (0.186) eV for Ti, V, Cr, and Mn, respectively. ACPF results are practically the same to MRCI+Q. At the C-MRCI (+Q) level the situation, on the average, becomes rather worse due to severe size nonextensivity errors: ΔE=0.140(0.049), 0.507 (0.328), 0.337 (0.205), and 0.471 (0.285) eV along the M series. It seems by now that, on the average and within the multireference CASSCF+1+2 approach, the best results between experimental and theoretical IPs are obtained at the MRCI-DK (+Q) level: Indeed, at this level ΔE=0.126(0.114), 0.027 (−0.065), 0.245 (0.192), and 0.268 (0.111) eV.

The numbers above show that the calculation of even atomic properties of the first row transition metal elements by first principle methods is not a trivial task.

Finally, the electron affinity (EA) of the fluorine atom in the CISD (+Q)/AQZ level is 3.03 (3.24) eV as compared to the experimental value of 3.40 eV.[42] It is of interest to note that even at the doubly augmented quadruple zeta CISD (+Q) level the F electron affinity does not improve, EA (dAQZ)=3.04 (3.25) eV, but the RCCSD(T)/AQZ value is 3.38 eV in excellent agreement with the experimental value.

IV. RESULTS AND DISCUSSION

Tables IV, V, VI, VII, and VIII list our numerical results for the ground and excited states of TiF, and VF, CrF, MnF, respectively. Potential energy curves (PEC) at the MRCI level of theory along with energy level diagrams (insets) are shown in Figs. 1–5.

A. TiF

Experimentally, the ground state of TiF was proposed to be of $^4\Sigma^-$ symmetry in 1969,[8] $X\,^2\Delta$ in 1985,[9] and finally $X\,^4\Phi$ in 1997[2] but based on unpublished MCSCF results of Harrison.[1] The most recent theoretical study by Boldyrev and

TABLE III. Absolute energies (E_h) and ionization potentials (eV) of Ti, V, Cr, and Mn in a variety of methods at the $[7s6p4d3f2g]$ basis set level.

Method	Ti(^3F)	Ti$^+$(^4F)←Ti(^3F)	V(^4F)	V$^+$(^5D) ←V(^4F)	Cr(^7S)	Cr$^+$(^6S)←Cr(^7S)	Mn(^6S)	Mn$^+$(^7S) ←Mn(^6S)
NHF[a]	−848.405 997	5.513	−942.884 337	5.811	−1 043.356 376	5.904	−1 149.866 251	
sa-SCF[b]	−848.405 776	5.519	−942.883 964	5.814	−1 043.355 898	5.907	−1 149.865 755	5.908
CASSCF[c]	−848.437 374	6.378	−942.886 264		−1 043.355 898	5.907	−1 149.877 769	6.235
MRCI	−848.463 251	6.658 (6.618)[j]	−942.960 116	6.390	−1 043.459 423	6.400	−1 150.004 810	7.096
MRCI+Q[d]	−848.463 788	6.669 (6.696)[j]	−942.965 348	6.503	−1 043.463 157	6.450	−1 150.012 302	7.248
MRACPF[e]	−848.463 523	6.664	−942.964 581	6.496	−1 043.462 029	6.439	−1 150.010 867	7.225
MRCI-DK[f]	−852.798 263	6.702	−948.211 604	6.719	−1 049.755 304	6.521	−1 157.516 289	7.166
MRCI-DK+Q[d]	−852.798 837	6.714	−948.216 038	6.809	−1 049.759 229	6.574	−1 157.524 039	7.323
C-MRCI[g]	−848.756 714	6.688 (6.412)[j]	−943.267 017	6.239	−1 043.784 212	6.429	−1 150.327 586	6.905
C-MRCI+Q[d]	−848.778 409	6.779 (6.629)[j]	−943.295 480	6.418	−1 043.812 240	6.561	−1 150.358 988	7.149
C-MRCI-DK	−853.141 766	6.722	−948.567 243	6.523	−1 050.130 072	6.539	−1 150.894 765	6.951
C-MRCI-DK+Q[d]	−853.166 488	6.817	−948.598 835	6.713	−1 050.161 061	6.680	−1 150.929 424	7.203
RCCSD(T)	−848.464 698	6.685 (6.690)[j]	−942.966 726	6.490	−1 043.464 750[k]	6.473	−1 150.013 456	7.261
RCCSD(T)-DK[f]	−852.799 735	6.730	−948.202 572	6.391			−1 157.525 411	7.338
C-RCCSD(T)[k]	−848.780 114	6.911 (6.914)[j]	−943.303 528	6.501	−1 043.822 88[k]	6.661	−1 150.371 430	7.317
C-RCCSD(T)-DK[f]	−853.169 775	6.961	−948.577 280	5.942			−1 157.944 734	7.397
Expt.[i]		6.828		6.746		6.766		7.434

[a]Numerical Hartree–Fock, Ref. 40.
[b]Spherically averaged SCF.
[c]Active space of Ti: $4s$, $4p$, $3d$ orbitals; active space of V, Cr, and Mn: $4s$, $4p_z$, $3d$ orbitals.
[d]+Q=the Davidson correction.
[e]Averaged coupled pair functional.
[f]+Douglas–Kroll relativistic corrections.
[g]The "core" $3s^2 3p^6$ electrons of Ti have been included in the CI procedure.
[h]$3s^2 3p^6$ electrons of Ti included.
[i]Reference 29.
[j]Ionization potentials at the correlation consistent-like $5z$ basis, Ref. 32.
[k]For technical reasons we were unable to calculate the Cr ^7S state at the RCCSD(T) level by the MOLPRO code; instead the ACES II code was used, Ref. 41.

Simons at the CCSD(T) level[25] (Table II), suggests a $^4\Phi$ ground state 0.08 eV (=645 cm^{-1}) lower than a $^4\Sigma^-$ state. The present results indicate rather clearly that the identity of the ground state of TiF is of $^4\Phi$ symmetry (*vide infra*).

All eight states studied correlate to the ground state atoms Ti($3d^2 4s^2, a\,^3F$)+F(^2P), Fig. 1. The ionization energy of Ti is 6.83 eV,[29] while the electron affinity of F is 3.40 eV,[42] therefore and within the M^+F^- bonding model, an "ionic avoided crossing" is expected with the incoming ionic state at around $r=((7.0-3.4)/27.2)^{-1}=7.6$ bohr, or about 4.0 Å. Indeed, this is the case for the entire MF series and all states examined, because the IP of Ti, V, Cr, and Mn atoms is about 7 eV (Ref. 29) (Figs. 1–5). Certainly, after 4 Å the bonding can be represented by the following valence-bond-Lewis (vbL) diagram, typified by the TiF molecule in the $^4\Phi$ state:

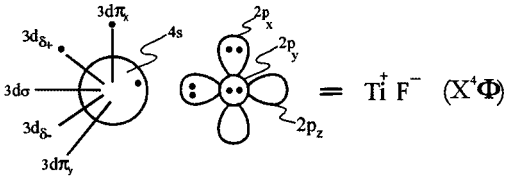

$$Ti^+(^4F;M_L=\pm 3)\quad F^-(^1S)$$

Clearly the three $3d^2 4s^1$ nonbonding (observer) electrons define the symmetry of the state. The equilibrium CASSCF configurations and the atomic Mulliken populations (Ti/F) are in complete agreement with the Scheme above, indicating a total transfer of about $0.8\,e^-$ from Ti to F,

$$|X\,^4\Phi\rangle_{B_1}=1/\sqrt{2}|(\text{core})^{20}1\sigma^2 2\sigma^2 3\sigma^1 1\pi_x^2 1\pi_y^2(2\pi_x^1 1\delta_+^1+2\pi_y^1 1\delta_-^1)\rangle$$
$$4s^{0.87}4p_z^{0.16}3d_{z^2}^{0.12}3d_{xz}^{0.51}3d_{yz}^{0.51}3d_{x^2-y^2}^{0.50}3d_{xy}^{0.50}/2s^{1.99}2p_z^{1.85}2p_x^{1.96}2p_y^{1.96},$$

where by $(\text{core})^{20}$ we mean the $1s^2 2s^2 2p^6 3s^2 3p^6$ and $1s^2\,e^-$ of Ti and F, respectively. Hereafter the common factor for all MF molecules and states, $(\text{core})^{20}1\sigma^2 2\sigma^2 1\pi_x^2 1\pi_y^2$ is omitted, therefore our kets will represent the M^+ valence electron distribution of M^+, $|M^+\rangle$. Within this notation the $|X\,^4\Phi\rangle$ configuration is written

$$|X\,^4\Phi\rangle_{B_1}=1/\sqrt{2}|3\sigma^1(2\pi_x^1 1\delta_+^1+2\pi_y^1 1\delta_-^1)\rangle. \quad (1)$$

Similarly, the leading CASSCF equilibrium CFs of the next seven examined states are

TABLE IV. Total energies E(hartree), equilibrium bond distances r_e (Å), dissociation energies D_e (kcal/mol), harmonic and anharmonic frequencies ω_e, $\omega_e x_e$ (cm^{-1}), rotational-vibrational constants α_e (cm^{-1}), dipole moments μ(D), effective charges q_{Ti}, and energy separations T_e (cm^{-1}) of TiF, $[7s6p4d3f2g/_{Ti}AQZ/_F]$ basis set.

Method	$-E$	r_e	D_e[a]	ω_e	$\omega_e x_e$	α_e	$\langle\mu\rangle/\mu_{FF}$[b]	q_{Ti}	T_e
				$X\ ^4\Phi$					
MRCI	948.301 64	1.863	130.7	639	3.7	0.0027	2.54/2.85	0.72	0.0
MRCI+Q[c]	948.320 55	1.860	131.9	641	3.8	0.0027			0.0
MRACPF[d]	948.318 01	1.861	130.4	638	6.1	0.0024	2.47	0.70	0.0
MRCI(+h)[e]	948.301 93	1.863	130.8	636	3.1	0.0025	2.56	0.70	0.0
MRCI-DK[f]	952.723 31	1.860	129.5	637	3.2	0.0025	2.51/2.81	0.81	0.0
MRCI-DK+Q[c]	952.742 35	1.857	130.7	637	2.9	0.0025			0.0
C-MRCI[g]	948.573 94	1.845	131.5	655	3.5	0.0023	2.48/2.95	0.74	0.0
C-MRCI+Q[c]	948.631 76	1.838	134.6	662	3.7	0.0023			0.0
C-MRCI-DK[f]	953.041 42	1.844	128.6	648	6.7	0.0026	2.47	0.82	0.0
C-MRCI-DK+Q[c,f]	953.103 14	1.837	131.7	653	6.0	0.0024			0.0
RCCSD(T)	948.323 19	1.875	129.1	641	6.8	0.0026	/2.95		0.0
C-RCCSD(T)[h]	948.643 15	1.839	132.0	649	3.2	0.0026	/2.80		0.0
Expt.[i]		1.831	136±8[j]	650.7($\Delta G_{1/2}$)		0.0026			
				$A\ ^4\Sigma^-$					
MRCI	948.297 01	1.843	128.8	626	2.8	0.0027	2.23/2.75	0.71	1015
MRCI+Q[c]	948.316 39	1.837	130.1	629	2.8	0.0028			913
MRACPF[d]	948.313 90	1.839	128.5	628	3.1	0.0026	2.26	0.69	902
MRCI(+h)[e]	948.297 30	1.843	128.9	628	2.9	0.0027	2.23	0.69	1016
MRCI-DK[f]	952.718 80	1.840	127.6	633	4.7	0.0027	2.21	0.80	990
MRCI-DK+Q[c]	952.738 33	1.835	128.9	633	3.3	0.0027			884
C-MRCI[g]	948.570 47	1.824	129.9	641	2.8	0.0025	2.13/2.80	0.73	761
C-MRCI+Q[c]	948.629 23	1.813	133.3	650	2.8	0.0026			555
C-MRCI-DK[f]	953.038 09	1.823	127.0	641			2.12	0.81	730
C-MRCI-DK+Q[c,f]	953.100 74	1.813	130.4	634					527
RCCSD(T)	948.321 46	1.842	128.0	654					380
C-RCCSD(T)[h]	948.642 74	1.789	131.7	699	3.3	0.0026	/3.00		90
				$B\ ^4\Pi$					
MRCI	948.291 14	1.875	124.5	620	3.8	0.0027	2.50/2.75	0.73	2305
MRCI+Q[c]	948.310 48	1.871	125.8	623	3.8	0.0027			2209
MRACPF[d]	948.308 04	1.872	124.3	611	2.8	0.0024	2.38	0.70	2187
MRCI(+h)[e]	948.291 43	1.874	124.6	617	3.0	0.0026	2.45	0.71	2306
C-MRCI[g]	948.563 51	1.855	125.2	630			2.45	0.74	2288
C-MRCI+Q[c]	948.621 92	1.847	128.6	637					2160
				$C\ ^4\Delta$					
MRCI	948.282 63	1.906	118.5	588	2.7	0.0024	1.91/1.88	0.73	4172
MRCI+Q[c]	948.301 97	1.902	119.9	590	2.8	0.0024			4078
MRACPF[d]	948.299 23	1.905	118.3	589	3.3	0.0024	1.81	0.70	4121
MRCI(+h)[e]	948.282 89	1.907	118.5	587	2.5	0.0024	1.91	0.72	4179
C-MRCI[g]	948.553 14	1.889	118.2	606			1.88	0.75	4565
C-MRCI+Q[c]	948.611 23	1.880	121.6	596					4507
				$a\ ^2\Delta$					
MRCI	948.281 33	1.799	117.6	617	2.9	0.0036	1.93/2.44	0.68	4458
MRCI+Q[c]	948.305 87	1.778	122.4	649	4.0	0.0041			3221
MRACPF[d]	948.302 87	1.778	120.5	651	6.8	0.0046	1.95	0.64	3323
MRCI(+h)[e]	948.281 66	1.798	117.7	618	3.8	0.0040	1.93	0.65	4451
C-MRCI[g]	948.551 16	1.783	117.0	633		0.0027	1.85	0.70	5001
C-MRCI+Q[c]	948.615 47	1.757	124.2	681		0.0044			3576
				$b\ ^2\Phi$					
MRCI	948.280 19	1.874	117.3	630	3.1	0.0026	2.19/2.54	0.72	4707
MRCI+Q[c]	948.300 01	1.872	119.0	621	2.8	0.0030			4508
MRACPF[d]	948.297 71	1.873	117.7	630	3.1	0.0025	2.26	0.69	4455
MRCI(+h)[e]	948.280 55	1.874	117.4	633	3.2	0.0025	2.19	0.70	4694
C-MRCI[g]	948.550 21	1.855	116.6	646		0.0023	2.10	0.73	5209
C-MRCI+Q[c]	948.608 64	1.849	120.1	650		0.0024			5074
				$c\ ^2\Sigma^-$					
MRCI	948.277 39	1.846	116.5	633	6.7	0.0040	1.68/1.78	0.70	5322
MRCI+Q[c]	948.297 89	1.840	118.5	650	4.1	0.0028			4973
MRACPF[d]	948.295 84	1.842	117.2	633	2.8	0.0026	1.69	0.68	4866
MRCI(+h)[e]	948.277 74	1.846	116.6	635	3.2	0.0027	1.68	0.68	5310
C-MRCI[g]	948.549 11	1.825	116.4	650			1.57	0.72	5450
C-MRCI+Q[c]	948.608 99	1.814	120.5	658					4998
				$d\ ^2\Pi$					
MRCI	948.271 81	1.878	112.4	618	3.2	0.0027	2.32/2.80	0.72	6547
MRCI+Q[c]	948.292 56	1.872	114.6	631	3.6	0.0024			6143
MRACPF[d]	948.290 51	1.873	113.3	619	3.1	0.0025	2.36	0.69	6036
MRCI(+h)[e]	948.272 15	1.877	112.5	619	3.0	0.0025	2.31	0.70	6536
C-MRCI[g]	948.541 96	1.859	111.7	635		0.0023	2.22	0.73	7019
C-MRCI+Q[c]	948.601 57	1.850	115.8	639		0.0023			6627

[a]With respect to the ground state atoms.
[b]$\langle\mu\rangle$ calculated as an expectation value, μ_{FF} obtained by the finite field method.
[c]+Q=the Davidson correction.
[d]Averaged coupled pair functional.
[e]An h ($l=5$) function has been added.
[f]+Douglas–Kroll relativistic corrections.
[g]The "core" $3s^2 3p^6$ electrons of Ti have been included in the CI procedure.
[h]$3s^2 3p^6$ of Ti included.
[i]See Table I.
[j]D_0.

TABLE V. Total energies E(hartree), equilibrium bond distances r_e (Å), dissociation energies D_e (kcal/mol),[a] harmonic and anharmonic frequencies ω_e, $\omega_e x_e$ (cm^{-1}), dipole moments μ(D), and energy separation T_e (cm^{-1}) of the TiF $X\,^4\Phi$ and $A\,^4\Sigma^-$ states, using the series of correlation consistent-type basis sets of Ti and the corresponding aug-cc-basis of F.[b]

Basis set	Method	$-E$	r_e	D_e	ω_e	$\omega_e x_e$	$\langle\mu\rangle/\mu_{FF}$	T_e
			$X\,^4\Phi$					
TZ/ATZ	MRCI	948.274 55	1.865	129.4	636	5.4	2.51/2.80	
	MRCI+Q[c]	948.292 27	1.862	130.4	634	2.9		
CTZ/ATZ	C-MRCI[d]	948.561 37	1.846	129.1	649	2.9	2.45/2.90	
	C-MRCI+Q[c]	948.618 03	1.839	132.0	654	2.9		
QZ/AQZ	MRCI	948.301 91	1.863	130.9	636	3.2	2.49/2.80	
	MRCI+Q[c]	948.320 78	1.859	132.1	638	3.3		
CQZ/AQZ	C-MRCI[d]	948.612 93	1.843	130.7	651	2.4	2.43/2.90	
	C-MRCI+Q[c]	948.674 10	1.836	134.0	657	2.9		
5Z/A5Z	MRCI	948.311 30	1.862	131.3	638	4.1	2.49/2.80	
	MRCI+Q[c]	948.330 50	1.859	132.6	639	4.0		
C5Z/A5Z	C-MRCI[d]	948.631 83	1.841	131.4	653	3.2	2.42/2.85	
	C-MRCI+Q[c]	948.694 35	1.834	134.8	659	2.6		
	C-MRCI-DK[e]	953.061 20	1.841	131.6			2.50	
	C-MRCI-DK+Q[c,e]	953.124 72	1.835	134.2				
CBS-limit	MRCI		1.861	131.6				
	MRCI+Q[c]		1.858	132.8				
	C-MRCI[d]		1.839	131.8				
	C-MRCI+Q[c]		1.833	135.3				
			$A\,^4\Sigma^-$					
5Z/A5Z	MRCI	948.306 69	1.841	129.4			2.17	1012
	MRCI+Q[c]	948.326 36	1.836	130.7				909
C5Z/A5Z	C-MRCI[d]	948.628 44	1.820	129.8			2.05	743
	C-MRCI+Q[c]	948.691 90	1.810	133.4				539
	C-MRCI-DK[e]	953.057 79	1.820	129.6			2.15	748
	C-MRCI-DK+Q[c,e]	953.122 15	1.812	132.6				564

[a]With respect to ground state products.
[b]See text.
[c]+Q=the Davidson correction.
[d]The "core" $3s^2 3p^6$ electrons of Ti are also correlated.
[e]+Douglas–Kroll relativistic corrections.

$$|A\,^4\Sigma^-\rangle_{A_2} = |0.82(3\sigma^1 1\delta_+^1 1\delta_-^1) - 0.57(3\sigma^1 2\pi_x^1 2\pi_y^1)\rangle, \tag{2}$$

$$|B\,^4\Pi\rangle_{B_1} = |0.65(3\sigma^1)(2\pi_x^1 1\delta_+^1 - 2\pi_y^1 1\delta_-^1) + 0.38(3\sigma^1 4\sigma^1 2\pi_x^1)\rangle, \tag{3}$$

$$|C\,^4\Delta\rangle_{A_2} = |3\sigma^1 4\sigma^1 1\delta_-^1\rangle, \tag{4}$$

$$|a\,^2\Delta\rangle_{A_2} = |0.78(3\sigma^2 1\delta_-^1) - 0.40(3\sigma^1 4\sigma^1 1\bar{\delta}_-^1) - 0.35(4\sigma^2 1\delta_-^1) - 0.31(3\sigma^1 4\bar{\sigma}^1 1\delta_-^1)\rangle, \tag{5}$$

$$|b\,^2\Phi\rangle_{B_1} = |0.61(3\sigma^1)(2\pi_x^1 1\bar{\delta}_+^1 - 2\bar{\pi}_y^1 1\delta_-^1) + 0.35(3\sigma^1)(2\bar{\pi}_x^1 1\delta_+^1 - 2\pi_y^1 1\bar{\delta}_-^1)\rangle, \tag{6}$$

$$|c\,^2\Sigma^-\rangle_{A_2} = |[0.66(3\sigma^1) + 0.38(3\sigma^1) + 0.32(4\bar{\sigma}^1)]1\delta_+^1 1\bar{\delta}_-^1 - 0.42(3\sigma^1 2\bar{\pi}_x^1 2\pi_y^1)\rangle, \tag{7}$$

$$|d\,^2\Pi\rangle_{B_1} \approx |0.56(3\sigma^1 2\pi_x^1 1\bar{\delta}_-^1) + 0.53(3\sigma^1 2\bar{\pi}_y^1 1\delta_-^1) + 0.36(3\sigma^1 4\bar{\sigma}^1 2\pi_x^1) + 0.34(3\sigma^1 2\pi_y^1 1\bar{\delta}_-^1) + 0.29(3\sigma^1 2\bar{\pi}_x^1 1\delta_+^1)\rangle. \tag{8}$$

1. $X\,^4\Phi$, $A\,^4\Sigma^-$

From Table IV we see that the MRCI (+Q) dissociation energy of TiF is $D_e = 130.7(131.9)$ kcal/mol or 130.4 kcal/mol at the MRACPF level. As we increase the level of calculation by adding core-correlation effects and DK-relativistic corrections, our formally "best" estimate for dissociation energy (D_e^*) is:

$$\begin{aligned} D_e^*(X\,^4\Phi) &= D_e(\text{MRCI}) + \{D_e(\text{C-MRCI}) - D_e(\text{MRCI})\} \\ &\quad + \{D_e(\text{C-MRCI-DK}) - D_e(\text{C-MRCI})\} \\ &\quad + \{D_e(\text{C-MRCI-DK+Q}) \\ &\quad - D_e(\text{C-MRCI-DK})\} + \text{BSSE} \\ &= D_e(\text{MRCI}) + \delta D_e(\text{core}) + \delta D_e(\text{DK}) \\ &\quad + \delta D_e(+\text{Q}) + \text{BSSE} \\ &= 130.7 + 0.8 + (-2.9) + 3.1 - 0.25 \\ &= 131.5 \ \text{kcal/mol}, \end{aligned} \tag{9}$$

a value which does not differ significantly from the "plain" MRCI result due to error cancellation.

Moving to Table V where the sequence of TZ/ATZ (CTZ/ATZ) to 5Z/A5Z (C5Z/A5Z) correlation consistent-

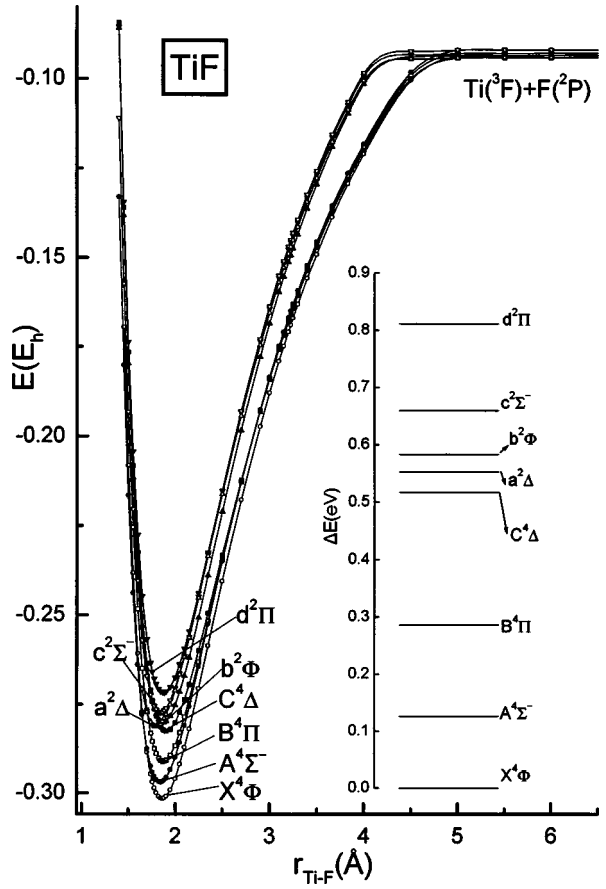

FIG. 1. MRCI potential energy curves of the TiF molecule. Energy level diagram inset. Energies have been shifted by +948.0 hartree.

type basis sets is used, and extrapolating to the CBS limit we obtain as before

$$
\begin{aligned}
&D_e(\mathrm{C5Z/A5Z}) \\
&\quad = D_e(\mathrm{MRCI})/(\mathrm{5Z/A5Z}) + \{D_e(\mathrm{C\text{-}MRCI}) - \mathrm{D}_e(\mathrm{MRCI})\} \\
&\qquad + \{D_e(\mathrm{C\text{-}MRCI\text{-}DK}) - D_e(\mathrm{C\text{-}MRCI})\} \\
&\qquad + \{D_e(\mathrm{C\text{-}MRCI\text{-}DK+Q}) - D_e(\mathrm{C\text{-}MRCI\text{-}DK})\} \\
&\qquad + \{D_e(\mathrm{C\text{-}MRCI/CBS}) - D_e(\mathrm{C\text{-}MRCI})\} \\
&\quad = D_e(\mathrm{MRCI})/(\mathrm{5Z/A5Z}) + \delta D_e(\mathrm{core}) + \delta D_e(\mathrm{DK}) \\
&\qquad + \delta D_e(+\mathrm{Q}) + \delta D_e(\mathrm{CBS}) = 131.3 + 0.1 + 0.2 + 2.6 \\
&\qquad + 0.4 = 134.2 + 0.4 = 134.6 \ \text{kcal/mol}, \qquad (10)
\end{aligned}
$$

an increase of 3.1 kcal/mol from the previous (D_e^*) value. A direct comparison between D_e(MRCI) and D_e(MRCI)/(5Z/A5Z) reveals, that by almost doubling the one-electron space (164 vs 305 functions), we lose just 0.1 kcal/mol at the C-MRCI level, but very interestingly the DK-relativistic effects become insignificant, +0.2 instead of −2.9 kcal/mol. Unfortunately, the rather large error bars of the experimentally determined $D_0 = 136 \pm 8$ kcal/mol,[5] does not allow for an easy comparison with our D_e^* or D_e(C5Z/A5Z) values. As a final comment on the dissociation energy we would like to add that the MRCI, C-MRCI values differ by +1.6 and −0.5 kcal/mol from the RCCSD(T) and C-RCCSD(T) values, respectively.

Concerning the bond distance, it decreases by 0.018 (0.025) Å by moving from MRCI to C-MRCI (+Q), obtaining $r_e = 1.845(1.838)$ Å at the latter level, in fair agreement with experiment. DK-relativistic effects seem to play no role in the determination of bond distance of TiF. Increasing the basis set to a final 5Z/A5Z (Table V) the CBS limit bond distance becomes 1.861 (1.838) [1.832] Å at the MRCI (C-MRCI) [C-MRCI+Q] level, converging monotonically to the experimental value. The RCCSD(T) r_e value is larger than the MRCI one by 0.012 Å, however it decreases by 0.036 Å at the C-RCCSD(T) level, twice as much than the corresponding decrease between the MRCI and C-MRCI values (0.018 Å), thus in excellent agreement with experiment. It is worth mentioning at this point that RCCSD(T) calculations based on CASSCF orbitals instead of HF, produce an $r_e = 1.863$ Å, identical to the MRCI r_e value.

Depending on the method, the ω_e values range from 637 (MRCI-DK) to 662 (C-MRCI+Q) cm^{-1}. At the C-MRCI level we obtain $\Delta G_{1/2} \equiv \omega_e - 2\omega_e x_e = 648\ \mathrm{cm}^{-1}$, just 2.7 cm^{-1} lower than the experimental one, or 647 using the corresponding C5Z/A5Z values of Table V.

The MRCI and C-MRCI dipole moments of the $X\,^4\Phi$ state calculated as expectation values ($\langle\mu\rangle$) are very close to 2.5 Debye, increasing to 2.9 D using the finite field method (μ_{FF}). We believe that the μ_{FF} values (2.95, 2.80 D at the C-MRCI and RCCSD(T), respectively) should be closer to "reality" than the $\langle\mu\rangle$ results (see also Ref. 43).

The leading CASSCF equilibrium configurations of the $A\,^4\Sigma^-$ state are given in Eq. (2). Table IV shows that as we increase the formal quality of the calculation, the $A\,^4\Sigma^- - X\,^4\Phi$ separation energy (T_e) decreases from 1015 (913) cm^{-1} to 730 (527) at the MRCI (+Q), C-MRCI-DK (+Q) levels, respectively. The results of DK relativistic effects on T_e are not significant, −25 (MRCI) and −30 (C-MRCI) cm^{-1}. In addition, we do not feel certain about the coupled clusters results predicting a $T_e = 90\ \mathrm{cm}^{-1}$ {C-RCCSD(T)}, due to the genuinely multireference character of the $^4\Sigma^-$ state [Eq. (2)]. Now at the C-MRCI-DK/(C5Z/A5Z) [+Q] level (Table V), we obtain $T_e = 748.4[564]\ \mathrm{cm}^{-1}$ in relative agreement with our previous numbers. Therefore, we can claim with enough confidence that the $X\,^4\Phi$ is the ground state of TiF, with the $A\,^4\Sigma^-$ state no more than 2 kcal/mol higher. Boldyrev and Simons[25] (Table II) obtained a $T_e(A\,^4\Sigma^- \leftarrow X\,^4\Phi) = 645\ \mathrm{cm}^{-1}$ at the UCCSD(T) level which should be contrasted to our RCCSD(T) [C-RCCSD(T)]=380 [90] cm^{-1} value (Table IV).

Obviously the binding energy of the $A\,^4\Sigma^-$ is practically the same to that of $X\,^4\Phi$ state, namely, very close to 130 kcal/mol. In detail, and carrying out the same analysis as before [Eq. (9)]

$$
\begin{aligned}
D_e^*(A\,^4\Sigma^-) &= D_e(\mathrm{MRCI}) + \delta D_e(\mathrm{core}) + \delta D_e(\mathrm{DK}) \\
&\quad + \delta D_e(+\mathrm{Q}) + \mathrm{BSSE} \\
&= 128.8 + 1.1 + (-2.9) + 3.4 - 0.25 \\
&= 130.2 \ \text{kcal/mol}.
\end{aligned}
$$

The dissociation energy in the C5Z/A5Z basis, and assuming the same δD_e(CBS) as in the $X\,^4\Phi$ state, becomes [Eq. (10)],

$$\begin{aligned} D_e(\mathrm{C5Z/A5Z}) &= D_e(\mathrm{MRCI})/(\mathrm{5Z/A5Z}) + \delta D_e(\mathrm{core}) \\ &\quad + \delta D_e(\mathrm{DK}) + \delta D_e(+\mathrm{Q}) \\ &\quad + \delta D_e(\mathrm{CBS}\text{-}X\,^4\Phi) \\ &= 129.4 + 0.4 \\ &\quad + (-0.2) + 3.0 + 0.4 \\ &= 132.6 + 0.4 = 133.0 \ \text{kcal/mol}. \end{aligned}$$

Note that using the C5Z/A5Z basis makes the DK-relativistic effects on D_e almost negligible (-0.2 kcal/mol).

2. $B^4\Pi$, $C^4\Delta$, $a^2\Delta$, $b^2\Phi$, $c^2\Sigma^-$, $d^2\Pi$

The equilibrium CASSCF configurations of these states are given in Eqs. (3)–(8), all of them but the $C\,^4\Delta$ being of multireference character. All states are strongly ionic conforming to the model Ti^+F^- with a total Mulliken charge transfer from Ti to F of about $0.7\,e^-$ (Table IV). Unfortunately no experimental data exist for any of these states.

At the highest level of calculation, C-MRCI (+Q), the $^4\Pi$ is the second excited state, 2288 (2160) cm^{-1} above the $X\,^4\Phi$ or 1527 (1605) cm^{-1} above the $A\,^4\Sigma^-$ state. At the same level of theory we obtain $D_e = 125.2(128.6)$ kcal/mol with respect to $\mathrm{Ti}(a\,^3F) + \mathrm{F}(^2P)$ and $r_e = 1.855(1.847)$ Å.

The next three excited states of $^4\Delta$, $^2\Delta$, and $^2\Phi$ symmetries tagged formally *C*, *a*, and *b*, respectively, span an energy range of about 2 kcal/mol (MRCI or C-MRCI), so their ordering is questionable. For instance, while the MRCI and C-MRCI ordering is maintained, at the MRCI+Q and C-MRCI+Q level the $^4\Delta$, $^2\Delta$ ordering is inverted.

For the next two calculated excited states, $c\,^2\Sigma^-$ and $d\,^2\Pi$, we are confident about their ordering having T_e values of 5450 (4998) and 7019 (6627) cm^{-1} at the C-MRCI (+Q) level, respectively.

Concluding the description of the TiF species, it can be said that the leading feature of all states studied is their overwhelming coulombic character, resulting to PECs of very similar morphology: In all states bond distances vary by no more than 0.11 Å, or 0.04 Å if we exclude the $C\,^4\Delta$ and $a\,^2\Delta$ states, while harmonic frequencies peak around 640 cm^{-1} within an energy range of 0.8 eV (Fig. 1).

B. VF

To the best of our knowledge there are only two experimental works in the literature on VF (Table I). In 1980 Jones and Krishnamurty[10] observed for the first time the emission spectrum of VF in the 3.4–3.6 eV (3660–3440 Å) region. By comparison with $\mathrm{CrO}(X\,^2\Pi)$,[44] isoelectronic to VF, it was suggested that the ground state of VF is of $^5\Pi$ symmetry.[10] In 2002, Bernath *et al.*,[11] by investigating the emission spectrum of VF in the 3400–17000 cm^{-1} region and by comparison with the isovalent species $\mathrm{VCl}(X\,^5\Delta)$,[45] proposed that the ground state of VF is of $^5\Delta$ symmetry, but they did not rule out the possibility of an $X\,^5\Pi$ state (see also Table I).

We are aware of only one theoretical work on VF published in 1989 by Averyanov and Khait.[26] These workers at a multireference CISD level obtained a $^5\Delta$ ground state with the $^5\Pi$ 1700 cm^{-1} higher (Table II). Our results indicate that the ground state of VF is a $^5\Pi$ with a $^5\Delta$ state 700–900 cm^{-1} higher (see below).

1. $X^5\Pi$, $A^5\Delta$

The equilibrium CASSCF configurations and corresponding Mulliken distributions of $X\,^5\Pi$ and $A\,^5\Delta$ states are

$$\begin{aligned} |X\,^5\Pi\rangle_{B_1} \approx & |0.86(3\sigma^1 2\pi_y^1 1\delta_+^1 1\delta_-^1) - 0.36(3\sigma^1 4\sigma^1) \\ & \times (2\pi_y^1 1\delta_-^1 + 2\pi_x^1 1\delta_+^1)\rangle \\ & \times 4s^{0.90} 4p_z^{0.20} 3d_{z^2}^{0.34} 3d_{xz}^{0.16} 3d_{yz}^{0.89} 3d_{x^2-y^2}^{0.87} 3d_{xy}^{0.87} / \\ & 2s^{1.96} 2p_z^{1.84} 2p_x^{1.95} 2p_y^{1.95} \end{aligned} \tag{11}$$

$$\begin{aligned} |A\,^5\Delta\rangle_{A_1} = & |3\sigma^1 2\pi_x^1 2\pi_y^1 1\delta_-^1\rangle \\ & \times 4s^{0.90} 4p_z^{0.17} 3d_{z^2}^{0.12} 3d_{xz}^{1.01} 3d_{yz}^{1.01} 3d_{x^2-y^2}^{1.00} / \\ & 2s^{1.97} 2p_z^{1.83} 2p_x^{1.96} 2p_y^{1.96}. \end{aligned} \tag{12}$$

A total charge transfer of about $0.7\,e^-$ from V to F is registered for both states conforming to the Coulombic M^+F^- model. Omitting the ''0.36'' components of the *X*-state, the ''bonding'' can be represented by the following vbL icons:

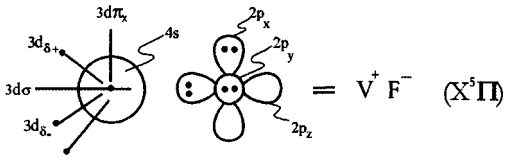

$V^+(^5F;M_L=\pm1)\quad F^-(^1S)$

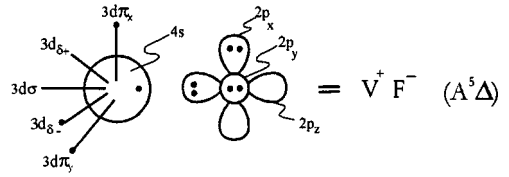

$V^+(^5F;M_L=\pm2)\quad F^-(^1S)$

Referring to Table VI the $X\,^5\Pi$ binding energy at the MRCI (+Q) level is $D_e = 126.2(127.9)$ kcal/mol; no experimental dissociation energy value exists up to now. As we increase the level of calculation, our ''best'' (D_e^*) estimate for D_e is [see also Eq. (9)]

$$\begin{aligned} D_e^*(X\,^5\Pi) &= D_e(\mathrm{MRCI}) + \delta D_e(\mathrm{core}) + \delta D_e(\mathrm{DK}) \\ &\quad + \delta D_e(+\mathrm{Q}) + \mathrm{BSSE} \\ &= 126.2 + 0.7 + (-3.2) + 3.5 - 0.29 \\ &= 126.9 \ \text{kcal/mol}, \end{aligned}$$

TABLE VI. Results on VF.[a]

Method	$-E$	r_e	D_e	ω_e	$\omega_e x_e$	α_e	$\langle\mu\rangle/\mu_{\mathrm{FF}}$	q_v	T_e
				$X\ ^5\Pi$					
MRCI	1 042.793 14	1.823	126.2	636	3.1	0.0028	2.31/2.77	0.66	0.0
MRCI+Q	1 042.815 29	1.815	127.9	644	3.3	0.0027			0.0
MRACPF	1 042.812 77	1.818	126.1	640	3.2	0.0027	2.26	0.64	0.0
MRCI(+h)	1 042.793 50	1.823	126.3				2.31	0.66	0.0
MRCI-DK	1 048.129 28	1.819	124.8	640	3.2	0.0027	2.28/2.72		0.0
MRCI-DK+Q	1 048.151 60	1.814	126.4	645	3.3	0.0027			0.0
C-MRCI	1 043.085 28	1.810	126.9	652	3.2	0.0027	2.27/2.82	0.69	0.0
C-MRCI+Q	1 043.146 70	1.800	130.5	662	3.4	0.0028			0.0
C-MRCI-DK	1 048.467 91	1.810	123.7	650	3.4	0.0027	2.27	0.79	0.0
C-MRCI-DK+Q	1 048.533 31	1.800	127.2	655	2.7	0.0028			0.0
RCCSD(T)	1 042.824 81	1.811	128.9	654	3.4	0.0028	/3.05		0.0
C-RCCSD(T)	1 043.166 26	1.788	131.8	674	3.4	0.0028	/3.25		0.0
Expt.[b]		1.7758		670.4	2.7	0.0028			
				$A\ ^5\Delta$					
MRCI	1 042.790 61	1.849	124.4	638	3.3	0.0026	2.69/3.19	0.69	557
MRCI+Q	1 042.812 04	1.845	125.5	639	3.2	0.0026			718
MRACPF	1 042.810 23	1.845	124.2	636	2.9	0.0025	2.62	0.67	557
MRCI(+h)	1 042.790 98	1.845	124.5				2.67	0.69	557
MRCI-DK	1 048.126 53	1.845	122.9	638	3.2	0.0025	2.66	0.78	605
MRCI-DK+Q	1 048.148 17	1.842	123.9	638	3.1	0.0027			758
C-MRCI	1 043.082 13	1.835	125.1	650	3.2	0.0025	2.62/3.20	0.70	694
C-MRCI+Q	1 043.142 56	1.830	128.0	655	2.6	0.0025			928
C-MRCI-DK	1 048.464 60	1.836	121.8	646	3.2	0.0026	2.63	0.80	726
C-MRCI-DK+Q	1 048.528 99	1.830	124.6	651	3.2	0.0026			952
RCCSD(T)	1 042.821 70	1.843	126.9	645	3.4	0.0026	/3.28		686
C-RCCSD(T)	1 043.162 53	1.826	129.4	657	3.8	0.0030	/3.38		815
				$B\ ^5\Sigma^-$					
MRCI	1 042.781 59	1.866	119.4	610	2.9	0.0025	2.27/2.08	0.69	2533
MRCI+Q	1 042.804 04	1.858	121.4	615	3.0	0.0025			2468
MRACPF	1 042.800 98	1.862	119.3	611	3.0	0.0025	2.01	0.66	2589
MRCI(+h)	1 042.781 93	1.865	119.5				2.26	0.69	2541
C-MRCI	1 043.073 32	1.854	119.4	622	3.0	0.0025	2.33	0.72	2621
C-MRCI+Q	1 043.134 98	1.843	123.1	629	2.8	0.0026			2589
				$a\ ^3\Pi$					
MRCI	1 042.769 72	1.825	111.5	645	3.1	0.0027	2.13/2.36	0.64	5138
MRCI+Q	1 042.793 21	1.818	114.0	648	3.1	0.0027			4847
MRACPF	1 042.790 99	1.818	112.5	645	3.1	0.0027	2.10	0.62	4783
MRCI(+h)	1 042.770 09	1.824	111.6				2.13	0.64	5138
C-MRCI	1 043.059 94	1.811	110.9	660	3.6	0.0029	2.10	0.66	5565
C-MRCI+Q	1 043.122 82	1.800	115.3	698		0.0011			5259
				$C\ ^5\Phi$					
MRCI	1 042.768 22	1.901	110.7	586	2.9	0.0025	2.36/2.39	0.71	5469
MRCI+Q	1 042.789 97	1.896	111.9	589	2.9	0.0025			5557
MRACPF	1 042.787 62	1.899	110.2	586	2.7	0.0024	2.20	0.68	5517
MRCI(+h)	1 042.768 56	1.901	110.7				2.35	0.71	5477
C-MRCI	1 043.059 30	1.889	110.9	595		0.0025	2.36	0.70	5702
C-MRCI+Q	1 043.120 03	1.881	112.9	599		0.0024			5872
				$b\ ^3\Sigma^-$					
MRCI	1 042.766 21	1.820	109.8	616	2.5	0.0023	2.25/2.50	0.63	5912
MRCI+Q	1 042.791 41	1.805	113.4	622	2.7	0.0023			5243
MRACPF	1 042.788 38	1.807	111.4	621	3.2	0.0025	2.21	0.61	5356
MRCI(+h)	1 042.766 58	1.819	109.8				2.24	0.63	5912
C-MRCI	1 043.056 66	1.805	108.9	630	2.8	0.0022	2.25		6275
C-MRCI+Q	1 043.121 56	1.785	114.6	637		0.0034			5541
				$c\ ^3\Delta$					
MRCI	1 042.763 05	1.857	107.1	633	3.1	0.0025	2.43	0.66	6606
MRCI+Q	1 042.785 41	1.854	108.8	634	3.1	0.0025			6557
MRACPF	1 042.784 06	1.855	107.8	631	2.6	0.0024	2.52	0.65	6299
MRCI(+h)	1 042.763 43	1.857	107.2				2.43	0.66	6598
C-MRCI	1 043.052 41	1.844	106.4	650		0.0020	2.35	0.67	7211
C-MRCI+Q	1 043.113 61	1.838	109.7	652		0.0011			7259
				$d\ ^3\Phi$					
MRCI	1 042.754 60	1.831	102.1	585	2.0	0.0025	2.57/3.36	0.65	8453
MRCI+Q	1 042.780 01	1.813	105.7	591	1.9	0.0029			7743
MRACPF	1 042.777 80	1.815	104.1	588	1.5	0.0027	2.63	0.62	7670
MRCI(+h)	1 042.754 97	1.830	102.2				2.56	0.64	8453
C-MRCI	1 043.044 22	1.817	101.4	601	2.0	0.0026	2.49	0.66	9009
C-MRCI+Q	1 043.109 14	1.793	107.0	615	3.5	0.0029			8267

[a]Symbols, units, and acronyms as in Table IV.
[b]See Table I.

in striking similarity with the corresponding TiF($X\,^4\Phi$) numerical corrections. Judging from the TiF($X\,^4\Phi$) binding energy where we gain 3.1 kcal/mol using the correlation consistent-type basis sets (5Z)+DK+CBS corrections with respect to D_e^*, we suggest that the D_e of $X\,^5\Pi$ is closer to 130 rather than 127 kcal/mol. Remarkably enough at the RCCSD(T) [C-RCCSD(T)] level, we obtain $D_e = 128.9[131.8]$ kcal/mol.

At the CI level the bond distance decreases monotonically from 1.823 (MRCI) to 1.810(C-MRCI) to 1.800 Å (C-MRCI+Q) with insignificant contributions from DK-relativistic effects, in fair agreement with the experimental value of 1.7758 Å.[11] The agreement is better at the C-RCCSD(T) level, where $r_e = 1.788$ Å (Table VI). All our ω_e values compare favorably with the experimental one, the largest discrepancy being 35 cm^{-1} (MRCI).

The $A\,^5\Delta$ state [Eq. (11)] is located 557 (718) cm^{-1} higher than the X-state at the MRCI (+Q) level of theory. Improving the quality of calculation the $T_e(A\,^5\Delta \leftarrow X\,^5\Pi)$ energy separation increases constantly to 694 (928) to 726 (952) cm^{-1} at the C-MRCI (+Q), C-MRCI-DK (+Q), respectively. We calculate basically the same T_e at the coupled cluster approach, 686 [815] cm^{-1} at the RCCSD(T) [C-RCCSD(T)], or 734 [847] cm^{-1} by adding the DK-effects as obtained from the MRCI, C-MRCI methods. Therefore, there is no doubt that the ground state of VF is a $^5\Pi$, with a $^5\Delta$ state located about 3 kcal/mol higher. The PECs of $X\,^5\Pi$ and $A\,^5\Delta$ states along with six more excited states (*vide infra*) and a level diagram for easy comparison are given in Fig. 2.

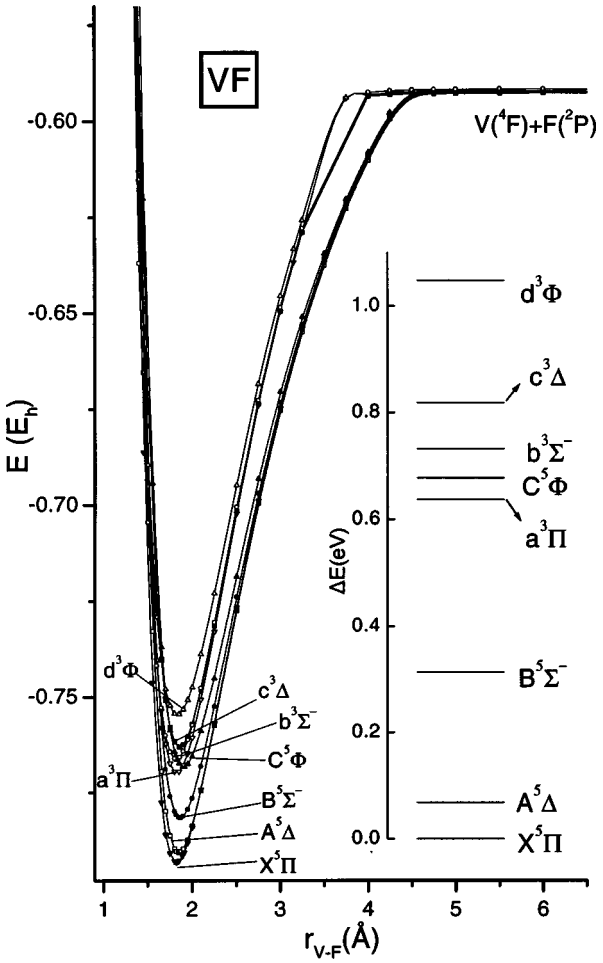

FIG. 2. MRCI potential energy curves of the VF molecule. Energy level diagram inset. Energies have been shifted by +1042.0 hartree.

2. $B^5\Sigma^-$, $a^3\Pi$, $C^5\Phi$, $b^3\Sigma^-$, $c^3\Delta$, $d^3\Phi$

The CASSCF equilibrium configurations of the two quintets are

$$|B\,^5\Sigma^-\rangle_{A_2} = |(3\sigma^1 4\sigma^1)[0.96(1\delta_+^1 1\delta_-^1) - 0.28(2\pi_x^1 2\pi_y^1)\rangle, \quad (13)$$

$$|C\,^5\Phi\rangle_{B_1} = |1/\sqrt{2}(3\sigma^1 4\sigma^1)(2\pi_x^1 1\delta_+^1 - 2\pi_y^1 1\delta_-^1)\rangle. \quad (14)$$

The four triplet states have ''genuine'' multireference character; we give below their leading CASSCF equilibrium configurations

$$|a\,^3\Pi\rangle_{B_1} \approx |0.62(3\sigma^1 2\pi_y^1 1\overline{\delta_+^1} 1\delta_-^1) + 0.35(3\sigma^1 2\overline{\pi_y^1} 1\delta_+^1 1\delta_-^1) - 0.26(3\sigma^2 2\pi_x^1 1\delta_+^1) + 0.27(4\sigma^1 2\pi_y^1 1\overline{\delta_+^1} 1\delta_-^1) + 0.26(3\sigma^1 2\pi_y^1 1\delta_+^1 1\overline{\delta_-^1})\rangle, \quad (15)$$

$$|b\,^3\Sigma^-\rangle_{A_2} \approx |0.71(3\sigma^1 4\sigma^1 1\overline{\delta_+^1} 1\delta_-^1) + [0.40(3\sigma^2) + 0.38(3\sigma^1 4\overline{\sigma^1})]1\delta_+^1 1\delta_-^1 + 0.30(3\sigma^1 4\sigma^1 1\delta_+^1 1\overline{\delta_-^1})\rangle, \quad (16)$$

$$|c\,^3\Delta\rangle_{A_2} = |0.81(3\sigma^1 2\pi_x^1 2\pi_y^1 1\overline{\delta_+^1}) + 0.46(3\sigma^1 2\overline{\pi_x^1} 2\pi_y^1 1\delta_+^1) + 0.33(3\sigma^1 2\pi_x^1 2\overline{\pi_y^1} 1\delta_+^1)\rangle, \quad (17)$$

$$|d\,^3\Phi\rangle_{B_1} \approx |1/\sqrt{4}3\sigma^2(2\pi_y^1 1\delta_-^1 + 2\pi_x^1 1\delta_+^1) + 3\sigma^1 4\sigma^1[0.37(2\pi_x^1 1\overline{\delta_+^1}) - 0.26(2\overline{\pi_y^1} 1\delta_-^1)] - 0.25(4\sigma^2)(2\pi_x^1 1\delta_+^1 + 2\pi_y^1 1\delta_-^1)\rangle. \quad (18)$$

All states correlate adiabatically to the ground state fragments, V($a\,^4F$)+F(^2P), conforming at the same time to the Coulombic binding model of V^+F^- after an interatomic distance of about 4 Å and towards equilibrium. There is no doubt that the second excited state is of $^5\Sigma^-$ symmetry, being 1976 (1927) [1661] cm^{-1} above the $A\,^5\Delta$ state at the MRCI (C-MRCI) [C-MRCI+Q] level of theory. According to our calculations the $a\,^3\Pi$ state is located 2605 cm^{-1} above the $B\,^5\Sigma^-$ state (MRCI) with a $^5\Phi$ state located nearby, the difference between the two latter states being 331 (137) [613] cm^{-1} at the MRCI (C-MRCI) [C-MRCI+Q] level. Obviously, and although the ordering between the $^3\Pi$ and $^5\Phi$ states is maintained at all levels of calculation, their small

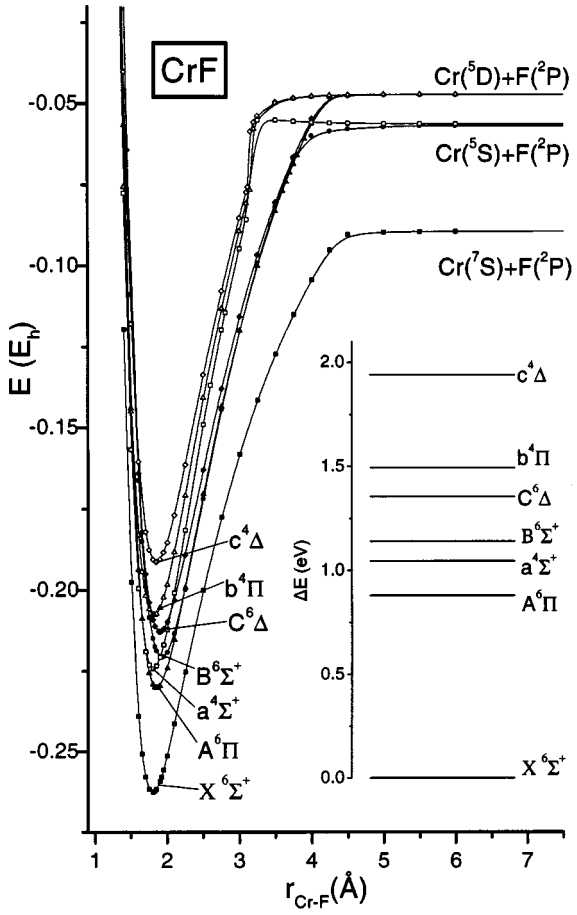

FIG. 3. MRCI potential energy curves of the CrF molecule. Energy level diagram inset. Energies have been shifted by +1143.0 hartree.

energy separation does not allow for a definite answer concerning their relative location. The same is true between the $C\,^5\Phi$ and $b\,^3\Sigma^-$ where their ordering is reversed moving from MRCI (C-MRCI) to MRCI+Q [C-MRCI+Q], Table VI. It seems that there is no doubt for the ordering of the $c\,^3\Delta$ and $d\,^3\Phi$ states at every level of calculation.

C. CrF

Rotational spectroscopy[13,16] indicates that the ground state of CrF is of $^6\Sigma^+$ symmetry in agreement with the best *ab initio* results of the literature by Harrison at the multireference level[27] (see also Tables I and II). Our results also clearly delineate a $^6\Sigma^+$ ground state with a $^6\Pi$ first excited state, approximately 0.9 eV higher. Table VII presents numerical results for a total of 7 states and Fig. 3 displays the MRCI potential energy curves and an energy level diagram.

1. $X^6\Sigma^+$

The equilibrium CASSCF configuration and the atomic Mulliken distributions are

$$|X\,^6\Sigma^+\rangle_{A_1} = 0.996|3\sigma^1 2\pi_x^1 2\pi_y^1 1\delta_+^1 1\delta_-^1\rangle$$
$$4s^{0.85}4p_z^{0.11}3d_{z^2}^{0.22}3d_{xz}^{1.01}3d_{yz}^{1.01}3d_{x^2-y^2}^{1.00}3d_{xy}^{1.00}/$$
$$2s^{1.98}2p_z^{1.82}2p_x^{1.96}2p_y^{1.96} \qquad (19)$$

(recall our convention of omitting the (core)[20] $1\sigma^2 2\sigma^2 1\pi^4$ factor, Sec. IV A). Approximately $0.7\,e^-$ are transferred from the metal to the $2p_z(2\sigma)$ orbital of the F atom. The Mulliken populations suggest that the *in situ* Cr^+ atom finds itself in a $^6D\,(4s^1 3d^4)$ state 1.52 eV (Ref. 29) higher than the ground $a\,^6S\,(3d^5)$ state of Cr^+. The bonding can be represented by the following vbL icon showing in essence the Cr^+ (^6D) atom in the field of the F^- anion.

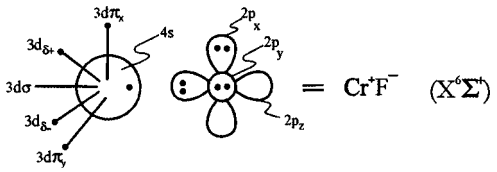

$$Cr^+(^6D;M_L=0) \qquad F^-(^1S)$$

The MRCI binding energy is 108.8 kcal/mol in agreement with the experimental value of $D_0 = 106.4 \pm 3.5$ kcal/mol (Ref. 6) (Table VII). Improving the level of calculation the D_e value increases monotonically to 110.2 kcal/mol (C-MRCI-DK+Q), or following the notation of Eq. (9), we write for the "best" (D_e^*) result

$$D_e^* = D_e(\mathrm{MRCI}) + \delta D_e(\mathrm{core}) + \delta D_e(\mathrm{DK}) + \delta D_e(+\mathrm{Q}) + \mathrm{BSSE}$$
$$= 108.8 + (-0.7) + (-2.1) + 4.2 - 0.29$$
$$= 109.9 \ \text{kcal/mol},$$

the largest positive increment caused by the Davidson correction and cancelling in essence the negative corrections. Our experience with the $X\,^4\Phi$ state of the TiF molecule shows that going to the CBS limit the "actual" D_e value is closer to 110 rather than 106 kcal/mol. At the C-RCCSD(T) level and applying the DK and BSSE corrections of the C-MRCI level we obtain, $D_e = 113.5 - 2.1 - 0.29 = 111$ kcal/mol, in practical agreement with D_e^*. Harrison's D_e value at the RCCSD(T) level obtained by the formula $D_e = E(\mathrm{CrF}) - [E(\mathrm{Cr}^+;{}^6S) - \mathrm{IP}_{\mathrm{expt}}(\mathrm{Cr}) + E(\mathrm{F}^-;{}^1S) + \mathrm{EA}_{\mathrm{expt}}(\mathrm{F})]$, where $\mathrm{IP}_{\mathrm{expt}}$ and $\mathrm{EA}_{\mathrm{expt}}$ are the experimental ionization potential and electron affinity of Cr and F, respectively, is 107.7 kcal/mol, as contrasted to our number of 113.4 kcal/mol using the same formula. This difference of 6 kcal/mol is the result of the smaller IP and EA by 6.8 and 0.5 kcal/mol of Cr and F obtained at the RCCSD(T) level as compared to the corresponding experimental values (Table III).

At the C-MRCI-DK or C-RCCSD(T) levels the bond distance is in complete agreement with the experimental value[13] and the same is true for the harmonic frequency (ω_e) in almost all computational levels.

2. $A^6\Pi$, $a^4\Sigma^+$, $B^6\Sigma^+$

Relatively recently experimental results have been published by Launila and co-workers for the sextets $^6\Pi$ (Refs. 14, 15) and $^6\Sigma^+$.[13] While there is no doubt by now that the

TABLE VII. Results on CrF.[a]

Method	$-E$	r_e	D_e[b]	ω_e	$\omega_e x_e$	α_e	$\langle\mu\rangle/\mu_{FF}$	q_{cr}	T_e
				$X\ ^6\Sigma^+$					
MRCI	1 143.262 59	1.800	108.8	655	4.4	0.0031	4.43/4.27	0.71	0.0
MRCI+Q	1 143.289 87	1.801	112.4	647	4.7	0.0033			0.0
MRACPF	1 143.288 41	1.804	111.6	633	4.0	0.0032	4.55	0.69	0.0
MRCI(+h)	1 143.263 32	1.799	108.9				4.43	0.70	0.0
MRCI-DK	1 149.649 77	1.788	109.2	684	3.3	0.0027	3.04/3.56	0.77	0.0
MRCI-DK+Q	1 149.675 39	1.783	112.1	688	3.3	0.0027			0.0
C-MRCI	1 143.569 37	1.792	108.1	666	4.3	0.0031	4.48/4.27	0.73	0.0
C-MRCI+Q	1 143.636 01	1.791	113.3	660	4.5	0.0032			0.0
C-MRCI-DK	1 150.002 20	1.783	106.0	689	3.4	0.0027	3.06	0.79	0.0
C-MRCI-DK+Q	1 150.070 33	1.777	110.2	696	3.8	0.0028			0.0
RCCSD(T)	1 143.298 25	1.797		662	4.6	0.0030	/4.35		0.0
C-RCCSD(T)	1 143.656 54	1.785		673	2.4	0.0028	/4.22		0.0
C-RCCSD(T)(+h)	1 143.662 30	1.783							0.0
Expt.[c]		1.7839	106.4±3.5[d]	664					
				$A\ ^6\Pi$					
MRCI	1 143.230 27	1.854	115.0	620	3.0	0.0025	2.34/2.41	0.69	7092
MRCI+Q	1 143.255 16	1.848	116.6	624	3.1	0.0026			7619
MRACPF	1 143.252 49	1.851	114.5	618	3.1	0.0026	2.24	0.66	7882
MRCI(+h)	1 143.230 91	1.852	115.0				2.33	0.69	7113
MRCI-DK	1 149.620 56	1.848	113.5	621	3.0	0.0027	2.28	0.77	6411
MRCI-DK+Q	1 149.645 76	1.842	115.0	625	3.1	0.0027			6503
C-MRCI	1 143.536 80	1.844	115.2	629	3.1	0.0026	2.37/2.47	0.71	7147
C-MRCI+Q	1 143.600 58	1.836	118.2	635	3.1	0.0026			7774
C-MRCI-DK	1 149.973 45	1.842	111.9	624	3.6	0.0031	2.34	0.79	6310
C-MRCI-DK+Q	1 150.041 01	1.834	114.8	634	3.8	0.0027			6435
RCCSD(T)	1 143.263 96	1.846		623	3.0	0.0026	/2.19		7525
RCCSD(T)-DK	1 149.653 35								7455
C-RCCSD(T)	1 143.620 32	1.832		637	3.2	0.0026	/2.16		7949
C-RCCSD(T)-DK	1 150.063 33								7515
C-RCCSD(T)(+h)	1 143.625 63	1.831							8047
Expt.[c]		1.8277		629					8134
				$a\ ^4\Sigma^+$					
MRCI	1 143.224 20	1.801	105.5	671	3.4	0.0027	2.00/2.41	0.64	8424
MRCI+Q	1 143.249 56	1.797	107.4	672	3.2	0.0027			8847
MRACPF	1 143.248 96	1.798	107.1	672	3.2	0.0027	2.29	0.62	8658
C-MRCI	1 143.528 56	1.792	104.5	685	3.4	0.0026	1.96/2.41	0.66	8957
C-MRCI+Q	1 143.592 34	1.785	107.7	690	3.4	0.0027			9583
				$B\ ^6\Sigma^+$					
MRCI	1 143.220 71	1.926	103.0	568	1.9	0.0020	3.38/3.61	0.78	9192
MRCI+Q	1 143.249 79	1.915	107.2	584	1.9	0.0019			8796
MRACPF	1 143.249 28	1.909	107.3	587	2.1	0.0020	2.70	0.71	8587
MRCI(+h)	1 143.221 42	1.925	102.9				3.37	0.77	9197
C-MRCI	1 143.525 78	1.920	102.4	573	1.9	0.0020	3.42	0.79	9567
C-MRCI+Q	1 143.593 86	1.908	108.1	590	2.0	0.0020			9250
Expt.[c]		1.8919		581					9953
				$C\ ^6\Delta$					
MRCI	1 143.212 80	1.897	104.0	587	2.9	0.0025	2.79/2.90	0.75	10927
MRCI+Q	1 142.236 61	1.894	104.7	587	2.9	0.0025			11689
MRACPF	1 143.234 90	1.896	103.1	584	2.9	0.0025	2.65	0.69	11744
C-MRCI	1 143.518 90	1.888	104.3	596	3.0	0.0025	2.79/2.90	0.73	11075
C-MRCI+Q	1 143.581 46	1.882	106.5	599	3.0	0.0025			11972
RCCSD(T)	1 143.244 96	1.892		588	2.8	0.0025	/2.69		11696
C-RCCSD(T)	1 143.600 51	1.880		599	3.1	0.0026	/2.64		12295
				$b\ ^4\Pi$					
MRCI	1 143.207 70	1.816	100.8	627	2.9	0.0023	2.33/2.82	0.64	12048
MRCI+Q	1 143.235 14	1.804	104.0	630	2.8	0.0023			12013
MRACPF	1 143.232 73	1.808	102.1	627	3.0	0.0025	2.36	0.62	12221
C-MRCI	1 143.512 47	1.806	99.9	637	2.7	0.0023	2.31/2.85	0.66	12488
C-MRCI+Q	1 143.579 09	1.790	104.6	641	2.5	0.0038			12492
				$c\ ^4\Delta$					
MRCI	1 143.191 30	1.850	90.6	593	2.2	0.0022	3.16/3.66	0.66	15646
MRCI+Q	1 143.217 98	1.839	93.0	591	1.9	0.0022			15778
MRACPF	1 143.216 80	1.839	91.7	591	2.1	0.0023	3.11	0.64	15716
C-MRCI	1 143.495 77	1.837	89.7	606	2.8	0.0024	3.12/3.66	0.68	16152
C-MRCI+Q	1 143.561 59	1.823	93.9	607	2.1	0.0023			16332

[a]Symbols, units, and acronyms as in Table IV.
[b]With respect to adiabatic fragments.
[c]See Table I.
[d]D_0.

first excited state is of $^6\Pi$ symmetry with the $^6\Sigma^+$ state about 2000 cm^{-1} higher (see below), for some reason the $^6\Sigma^+$ state was tagged as $A\,^6\Sigma^+$ and the $^6\Pi$ as $B\,^6\Pi$.[13,14] In the present work we follow what seems to be the standard empirical nomenclature,[46] namely, $A\,^6\Pi$ and $B\,^6\Sigma^+$ (Fig. 3).

The equilibrium CASSCF configurations for the states above are

$$|A\,^6\Pi\rangle_{B_1} = 0.997|3\sigma^1 4\sigma^1 2\pi_y^1 1\delta_+^1 1\delta_-^1\rangle, \tag{20}$$

$$\begin{aligned}|a\,^4\Sigma^+\rangle_{A_1} = |&3\sigma^1[0.79(2\pi_x^1 2\pi_y^1 1\overline{\delta}_+^1 1\delta_-^1)\\ &+0.45(2\overline{\pi}_x^1 2\pi_y^1 1\delta_+^1 1\delta_-^1)]\\ &+3\sigma^1[0.32(2\pi_x^1 2\overline{\pi}_y^1 1\delta_+^1 1\delta_-^1)\\ &+0.25(2\pi_x^1 2\pi_y^1 1\delta_+^1 1\overline{\delta}_-^1)]\rangle,\end{aligned} \tag{21}$$

$$|B\,^6\Sigma^+\rangle_{A_1} = 0.995|4\sigma^1 2\pi_x^1 2\pi_y^1 1\delta_+^1 1\delta_-^1\rangle. \tag{22}$$

For these states, as in all molecules and states presently studied, about $0.7\,e^-$ are transferred from the metal atom to $2p_z(2\sigma)$ of the F atom around the equilibrium geometry.

The $A\,^6\Pi$ state arises from the $X\,^6\Sigma^+$ state by moving a $2\pi_x(=3d\pi_x)$ electron to a $4\sigma[\approx(0.65)(3d\sigma-4s)+(0.17)4p_z]$ orbital. As seen from Fig. 3, the $A\,^6\Pi$ state traces its origin to the second excited state of $Cr(3d^4 4s^2; a\,^5D)$, 8118 cm^{-1} higher[29] than the ground ^7S of Cr. However, at the equilibrium the *in situ* Cr^+ finds itself in the $^6D(4s^1 3d^4)$ state as revealed by the Mulliken distributions, $4s^{0.90}4p_z^{0.25}3d_{z^2}^{1.01}3d_{xz}^{0.03}3d_{yz}^{1.02}3d_{x^2-y^2}^{1.0}3d_{xy}^{1.0}$. At the highest level of calculation (C-MRCI-DK+Q) $D_e^*(A\,^6\Pi) = D_e(\mathrm{MRCI}) + \delta D_e(\mathrm{core}) + \delta D_e(\mathrm{DK}) + \delta D_e(+\mathrm{Q}) + \mathrm{BSSE} = 115.0 + 0.2 + (-3.3) + 2.9 - 0.30 = 114.8 - 0.30 = 114.5$ kcal/mol with respect to $Cr(^5D)+F(^2P)$ fragments, at $r_e = 1.834$ Å. The latter value is in good agreement with the experimental value of 1.8277 Å.[15] Assuming that the DK-effects in both C-MRCI and C-RCCSD(T) methods affect the internuclear distance similarly, at the C-RCCSD(T)$(+h)$ level we obtain $r_e = 1.831 - 0.002 = 1.829$ Å, now in complete agreement with the experimental value.

It is interesting to follow the behavior of the different computational approaches concerning the $A\,^6\Pi - X\,^6\Sigma^+$ energy separation. Experimentally,[15] $T_e(A\,^6\Pi \leftarrow X\,^6\Sigma^+) = 8134\,cm^{-1}$. At the MRCI+Q or MRACPF level the agreement is more than fair (Table VII), considering the inherent difficulties of these systems. At the C-MRCI+Q, $T_e = 7774\,cm^{-1}$ just 1 kcal/mol smaller than the experimental value, and we surmise that approximately the same results would have been obtained at the C-MRACPF level. However, the addition of DK relativistic effects is problematic, reducing the T_e with respect to MRCI and C-MRCI values by 681 and 837 cm^{-1}, respectively. More or less similar trends are reported in Ref. 27, but in conjunction with the Cowan–Griffin relativistic approach. Clearly, the best results are obtained at the C-RCCSD(T) [C-RCCSD(T)$(+h)$] level, where $T_e = 7949[8047]\,cm^{-1}$ in complete agreement with experiment. We are reminded that the $X\,^6\Sigma^+$ and $A\,^6\Pi$ are single reference states [Eqs. (19) and (20)], therefore adequately described by the CC-approach. The addition of DK-effects on the RCCSD(T) and C-RCCSD(T) is rather detrimental to the T_e value being 7455 and 7515 cm^{-1}, respectively.

The $a\,^4\Sigma^+$ state, a truly multireference state [Eq. (21)], correlates adiabatically to a $Cr(^5S)$ 0.941 eV above the ^7S Cr ground state[29] (Fig. 3). In equilibrium, the CASSCF Mulliken distributions are (Cr/F)

$$4s^{0.94}4p_z^{0.18}3d_{z^2}^{0.11}3d_{xz}^{1.02}3d_{yz}^{1.02}3d_{x^2-y^2}^{1.00}3d_{xy}^{1.00}/$$
$$2s^{1.95}2p_z^{1.80}2p_x^{1.96}2p_y^{1.96}$$

pointing to a $4s^1 3d^4$ *in situ* Cr^+ configuration of ^4D atomic symmetry, 2.458 eV (Ref. 29) higher than the ground $a\,^6S$ state of Cr^+. No experimental results are available for this state. At the highest level (C-MRCI+Q), we calculate $D_e = 104.5(107.7)$ kcal/mol at $r_e = 1.792(1.785)$ Å, and $T_e(a\,^4\Sigma^+ \leftarrow X\,^6\Sigma^+) = 8957(9583)\,cm^{-1}$, very close to the $B\,^6\Sigma^+$ state (but see below).

The (formally) $B\,^6\Sigma^+$ state correlates also to the $Cr(^5S)+F(^2P)$ atomic fragments with its CASSCF equilibrium configurations given in Eq. (22). Its Mulliken equilibrium distributions are

$$4s^{0.09}4p_z^{0.20}3d_{z^2}^{0.82}3d_{xz}^{1.01}3d_{yz}^{1.01}3d_{x^2-y^2}^{1.00}3d_{xy}^{1.00}/$$
$$2s^{2.0}2p_z^{1.88}2p_x^{1.97}2p_y^{1.97}$$

dictating a a $^6S(3d^5)$ *in situ* Cr^+ state. This is also clear from the composition of the 4σ orbital $(\approx(0.86)d\sigma+(0.29)4s)$, practically of d_{z^2} character. Moving from MRCI to C-MRCI+Q the bond distance converges monotonically to a final value of $r_e = 1.908$ Å, in acceptable agreement with the experimental value of 1.8916 Å.[13] Concerning the $T_e(B\,^6\Sigma^+ \leftarrow X\,^6\Sigma^+)$ energy gap, the MRCI (C-MRCI) values are 9192 (9567) cm^{-1} in very good agreement with the experimental value[13] of 9953 cm^{-1}. At this level of theory the ordering of $a\,^4\Sigma^+$ and $B\,^6\Sigma^+$ is maintained with the $B\,^6\Sigma^+$ being higher by 768 (610) cm^{-1}. The addition of Davidson correction (+Q) reduces the $T_e(B\,^6\Sigma^+ \leftarrow X\,^6\Sigma^+)$ by 396 and 317 cm^{-1} at the MRCI+Q and C-MRCI+Q, respectively. Exactly the opposite is happening in the $a\,^4\Sigma^+$ state by 423 and 626 cm^{-1} (Table VII). The net result is the *inversion* of the two states at the MRCI+Q and C-MRCI+Q levels, with the $a\,^4\Sigma^+$ state now *higher* by 51 (MRCI+Q) and 333 (C-MRCI+Q) cm^{-1}. Therefore, within the accuracy of our calculations, the $a\,^4\Sigma^+$ and $B\,^6\Sigma^+$ states should be considered as degenerate. Practically the same conclusions have been reached by Harrison[27] concerning the ordering of $a\,^4\Sigma^+$ and $B\,^6\Sigma^+$ states.

3. $C^6\Delta$, $b^4\Pi$, $c^4\Delta$

All three states correlate adiabatically to $Cr(^5D)+F(^2P)$ (Fig. 3). The main equilibrium CASSCF configurations and atomic Mulliken populations (Cr/F) are as follows:

$$|C\,^6\Delta\rangle_{A_1}=0.997|3\sigma^1 4\sigma^1 2\pi_x^1 2\pi_y^1 1\delta_-^1\rangle,\ 4s^{0.91}4p_z^{0.24}3d_{z^2}^{1.01}3d_{xz}^{1.01}3d_{yz}^{1.01}3d_{x^2-y^2}^{1.00}/2s^{1.97}2p_z^{1.85}2p_x^{1.96}2p_y^{1.96}, \quad (23)$$

$$|b\,^4\Pi\rangle_{B_1}=|[(0.68)3\sigma^2-(0.45)4\sigma^2]2\pi_y^1 1\delta_+^1 1\delta_-^1-3\sigma^1 4\sigma^1[(0.38)2\pi_y^1 1\bar{\delta}_+^1 1\delta_-^1+(0.29)2\bar{\pi}_y^1 1\delta_+^1 1\delta_-^1$$
$$+(0.24)2\pi_y^1 1\delta_+^1 1\bar{\delta}_-^1]\rangle,\ 4s^{1.02}4p_z^{0.19}3d_{z^2}^{1.00}3d_{xz}^{0.04}3d_{yz}^{1.02}3d_{x^2-y^2}^{1.00}3d_{xy}^{1.00}/2s^{1.95}2p_z^{1.83}2p_x^{1.94}2p_y^{1.95}, \quad (24)$$

$$|c\,^4\Delta\rangle_{A_2}=|[(0.73)3\sigma^2-(0.42)4\sigma^2]2\pi_x^1 2\pi_y^1 1\delta_+^1+3\sigma^1 4\sigma^1 2\pi_y^1[(0.41)2\pi_x^1 1\bar{\delta}_+^1$$
$$+(0.28)2\bar{\pi}_x^1 1\delta_+^1]\rangle,\ 4s^{1.06}4p_z^{0.16}3d_{z^2}^{0.99}3d_{xz}^{1.02}3d_{yz}^{1.02}3d_{x^2-y^2}^{1.00}/2s^{1.95}2p_z^{1.82}2p_x^{1.96}2p_y^{1.96}. \quad (25)$$

A total of approximately $0.7e^-$ migrates from Cr to the $2p_z(2\sigma)$ orbital of the F atom. In the $C\,^6\Delta$ state the Cr^+ finds it self in the first excited $a\,^6D(3d^4 4s^1)$ state, while in the $b\,^4\Pi$ and $c\,^4\Delta$ states the *in situ* Cr^+ is in its second excited $a\,^4D(3d^4 4s^1)$ state.

With respect to the adiabatic fragments the binding energies at the C-MRCI+Q level for the $C\,^6\Delta$, $b\,^4\Pi$, and $c\,^4\Delta$ states are 106.5, 104.6, and 93.9 kcal/mol, respectively, at corresponding equilibrium distances of 1.882, 1.790, and 1.823 Å. The D_e differences between the states are equal to the $T_e(b\,^4\Pi\leftarrow C\,^6\Delta)$, $T_e(c\,^4\Delta\leftarrow b\,^4\Pi)$ values because all three states correlate to the same atomic fragments. No experimental results are available for these states.

D. MnF

No theoretical results of any kind have been reported in the literature to the present time on MnF. According to Sheridan and Ziurys,[47] the earliest spectroscopic observation of MnF goes back to 1939,[48] where two band systems were observed. From the ESR spectrum of MnF,[49] it was concluded that the radical is best described as Mn^+F^-, and this is in accord with a $^7\Sigma$ ground state, since the Mn^+ cation is described by an $a\,^7S(3d^5 4s^1)$ term.[29] To our understanding the ESR experimental results of Ref. 49 is the only direct evidence of the ground state symmetry of MnF until now. Our calculations also leave no doubt that MnF has a $^7\Sigma^+$ ground state (*vide infra*). All relative experimental information on MnF pertaining to the present work is collected in the last entry of Table I.

1. $X^7\Sigma^+$, $a^5\Sigma^+$

Both the *X*- and *a*-states correlate adiabatically to the ground state atoms $Mn(3d^5 4s^2; a\,^6S)+F(^2P)$, Fig. 4. The leading equilibrium CASSCF configurations and Mulliken populations are

$$|X\,^7\Sigma^+\rangle_{A_1}=0.997|3\sigma^1 4\sigma^1 2\pi_x^1 2\pi_y^1 1\delta_+^1 1\delta_-^1\rangle$$
$$\times 4s^{0.93}4p_z^{0.26}3d_{z^2}^{1.01}3d_{xz}^{1.01}3d_{yz}^{1.01}3d_{x^2-y^2}^{1.01}3d_{xy}^{1.00}/$$
$$2s^{1.96}2p_z^{1.85}2p_x^{1.96}2p_y^{1.96}, \quad (26)$$

where

$$3\sigma\approx(0.62)4s+(0.67)3d\sigma,$$

$$4\sigma\approx(0.64)4s-(0.72)3d\sigma,$$

and

$$|a\,^5\Sigma^+\rangle_{A_1}$$
$$\approx|[(0.64)3\sigma^2-(0.46)4\sigma^2]2\pi_x^1 2\pi_y^1 1\delta_+^1 1\delta_-^1$$
$$+3\sigma^1 4\sigma^1 2\pi_y^1 1\delta_-^1[(0.38)2\pi_x^1 1\bar{\delta}_+^1$$
$$+(0.30)2\bar{\pi}_x^1 1\delta_+^1]\rangle \quad (27)$$

with $3\sigma\approx-(0.62)4s+(0.67)3d\sigma$, $4\sigma\approx(0.57)4s+(0.71)3d\sigma$. As in all states and MF species studied here, about $0.7e^-$ are transferred from the metal to the $2p_z=(2\sigma)$ orbital of the F atom. Clearly, the *in situ* Mn^+ ion finds itself in the $a\,^7S(3d^5 4s^1)$ and $a\,^5S(3d^5 4s^1)$ states for the $X\,^7\Sigma^+$ and $a\,^5\Sigma^+$ molecular states, respectively. The ^5S is the first excited state of Mn^+, 1.174 eV above the ^7S

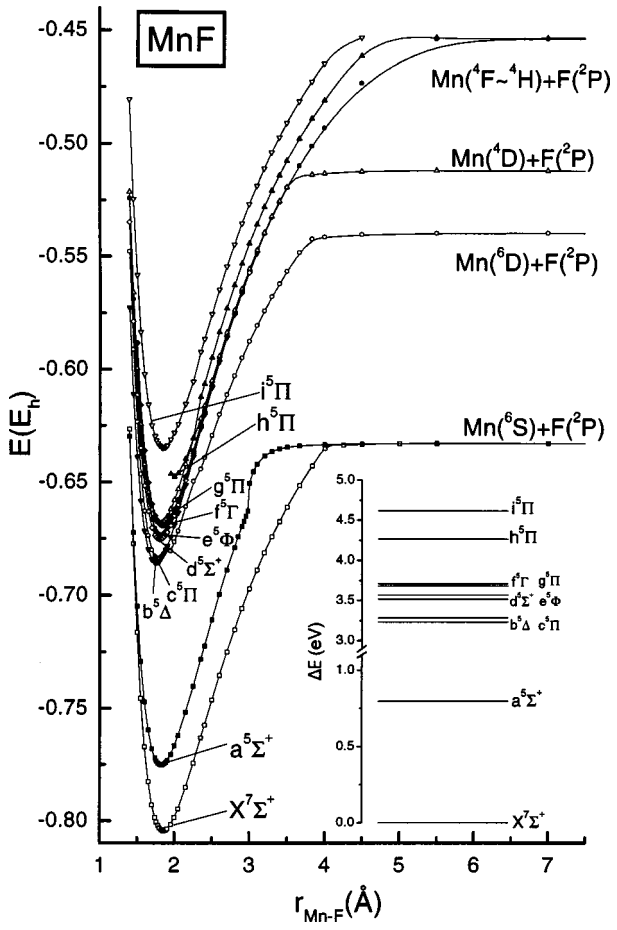

FIG. 4. MRCI potential energy curves of the MnF molecule. Energy level diagram inset. Energies have been shifted by +1249.0 hartree.

state.[29] Taking into account that the bonding is identical in both states, pictorially described by the following vbL diagram in the case of high spin,

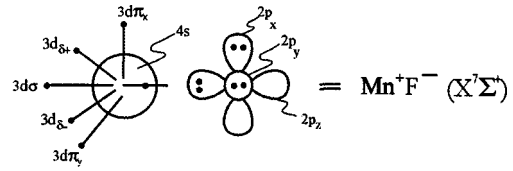

$$Mn^{+}(^{7}S;M_L=0)\quad F^{-}(^{1}S)$$

the $^5S-^7S$ atomic splitting reflects the corresponding $a\,^5\Sigma^+-X\,^7\Sigma^+$ molecular *ab initio* splitting of about 0.8 eV (see below).

The spin-forbidden $a\,^5\Sigma^+\leftarrow X\,^7\Sigma^+$ transition makes the experimental determination of the $a-X$ separation difficult. Launila and Simard using laser-induced fluorescence spectroscopy,[18] give an *indirectly* obtained estimate of about 3000 ± 1000 cm^{-1}. As they say,[18] ''this estimate, together with considerations involving similar situations with the same setup, indicates that the energy separation between $X\,^7\Sigma^+$ and $a\,^5\Sigma^+$ is likely to be 3000 ± 1000 cm^{-1}.'' In a subsequent paper by Launila and co-workers[20] this number is modified to 3500 ± 1000 cm^{-1}. In a more recent experimental work using chemiluminescence spectroscopy and reaction energetics,[22] it is suggested that the $a-X$ splitting is 2500 ± 1000 cm^{-1} (see also Table I).

Our *ab initio* results imply that the $a-X$ energy gap is about twice as large than the ''experimental'' values. MRCI (MRCI-DK) and C-MRCI (C-MRCI-DK) calculations predict similar values, namely 6435 (6540) and 6855 (7030) cm^{-1}, respectively (Table VIII). At the RCCSD(T) and C-RCCSD(T) levels these numbers become 6714 and 8299 cm^{-1}, but we have to remember that the $a\,^5\Sigma^+$ state requires a multireference description [Eq. (27)], not provided by the single reference CC-approach used here. Therefore, and taking into account the Davidson correction, our best estimate for the $a\,^5\Sigma^+-X\,^7\Sigma^+$ energy separation, is bracketed between 6500 and 7000 cm^{-1}.

Experimentally, the binding energy D_0 of the $X\,^7\Sigma^+$ state varies from 101.2 to 104.5 to 106.4 kcal/mol, all thermochemically determined (Table I). Irrespective of the method of calculation, our D_e values are in excellent agreement with the most recent experimental value, $D_0=106.4\pm1.8$ kcal/mol;[23] or using the same conventions as in Eq. (9), $D_e^*(X\,^7\Sigma^+)=D_e(\mathrm{MRCI})+\delta D_e(\mathrm{core})+\delta D_e(\mathrm{DK})+\delta D_e(+\mathrm{Q})+\mathrm{BSSE}=107.8+0.9+(-3.9)+2.1-0.38=106.5$ kcal/mol. At the C-MRCI-DK+Q level the bond distance differs by just 0.003 Å from the experimental one[20] (Table VIII).

The C-MRCI-DK+Q binding energy of the $a\,^5\Sigma^+$ state is 88 kcal/mol (89.4 kcal/mol at the MRCI level) with respect to ground state products, at $r_e=1.803$ Å, in contrast to the experimental value of 1.7854 Å.[18] However, the intrinsic bond strength, i.e., with respect to the diabatic fragments $Mn^+(^5S)+F^-(^1S)$, is $88+\mathrm{IP(Mn)}-\mathrm{EA(F)}+\Delta E(Mn^+;{}^5S\leftarrow{}^7S)=88$ kcal/mol$+7.432$ eV-3.40 eV$+1.174$ eV$=208$ kcal/mol, using the experimental ionization potential of Mn and electron affinity of F. *Mutatis mutandis* the intrinsic bond strength of the $X\,^7\Sigma^+$ state is 106.9 kcal/mol$+7.432$ eV -3.40 eV$=200$ kcal/mol. This analysis shows that the Mn–F binding energy is stronger in the $a\,^5\Sigma^+$ state albeit by 8 kcal/mol, while the binding energy with respect to ground state products is larger in the $X\,^7\Sigma^+$ by 19 kcal/mol. This, somehow, is reflected in the much shorter (by 0.05 Å) bond distance of the $a\,^5\Sigma^+$ state and its larger harmonic frequency (by 22 cm^{-1}), as compared to the X-state (Table VIII).

2. $b^5\Delta$, $c^5\Pi$, $d^5\Sigma^+$, $e^5\Phi$, $f^5\Gamma$, $g^5\Pi$

The manifold of these six quintets is located approximately 2.7 eV above the $a\,^5\Sigma^+$ state, spanning an energy range of less than 0.5 eV (Fig. 4). At the MRCI (C-MRCI) the energy separations between the states ($b\,^5\Delta$,$c\,^5\Pi$), ($d\,^5\Sigma^+$,$e\,^5\Phi$), and ($f\,^5\Gamma$,$g\,^5\Pi$) tagged formally according to the MRCI approximation, are 419 (280), 430 (140), and 210 (525) cm^{-1}, respectively. It is obvious that the ordering of these states within each pair is uncertain, and indeed, at the +Q level the $f\,^5\Gamma$, $g\,^5\Pi$ ordering is inverted, becoming -420 (-280) cm^{-1} (Table VIII). In what follows we give the dominant equilibrium CASSCF configurations of the six quintets above.

$$|b\,^5\Delta\rangle_{A_1}\approx|3\sigma^1 2\pi_x^1 2\pi_y^1 1\delta_-^1[(0.77)1\delta_+^2-(0.29)4\sigma^2]\rangle, \tag{28}$$

$$|c\,^5\Pi\rangle_{B_1}\approx|[(0.72)3\sigma^2+(0.55)4\sigma^2]2\pi_x^1 2\pi_y^1 1\delta_+^1 1\delta_-^1\rangle, \tag{29}$$

$$\begin{aligned}|d\,^5\Sigma^+\rangle_{A_1}\approx|&3\sigma^1 4\sigma^1[(0.64)2\bar{\pi}_x^1 2\pi_y^1\\&+(0.50)2\pi_x^1 2\bar{\pi}_y^1]1\delta_+^1 1\delta_-^1+[(0.37)3\sigma^2\\&-(0.40)3\sigma^1 4\bar{\sigma}^1]2\pi_x^1 2\pi_y^1 1\delta_+^1 1\delta_-^1\rangle,\end{aligned} \tag{30}$$

$$\begin{aligned}|e\,^5\Phi\rangle_{B_1}\approx|&(0.58)3\sigma^1 4\sigma^1(2\pi_y^1 1\delta_+^2 1\delta_-^1\\&+2\pi_x^1 1\delta_+^1 1\delta_-^2)\\&+(0.40)3\sigma^1 4\sigma^1(2\pi_x^2 2\pi_y^1 1\delta_-^1\\&+2\pi_x^1 2\pi_y^2 1\delta_+^1)\rangle,\end{aligned} \tag{31}$$

$$\begin{aligned}|f\,^5\Gamma\rangle_{A_1}\approx&0.77|3\sigma^1 4\sigma^1 2\pi_x^1 2\pi_y^1 1\delta_+^1 1\bar{\delta}_-^1\rangle\\&+|[(0.50)3\bar{\sigma}^1 4\sigma^1\\&+(0.29)3\sigma^1 4\bar{\sigma}^1]2\pi_x^1 2\pi_y^1 1\delta_+^1 1\delta_-^1\rangle,\end{aligned} \tag{32}$$

$$\begin{aligned}|g\,^5\Pi\rangle_{B_1}\approx|&(0.60)3\sigma^1 4\sigma^1(2\pi_x^1 1\delta_+^1 1\delta_-^2\\&+2\pi_y^1 1\delta_+^2 1\delta_-^1)\rangle\\&+0.37|3\sigma^2 4\sigma^1 2\pi_y^1 1\delta_+^1 1\delta_-^1\rangle.\end{aligned} \tag{33}$$

With the exception of the $f\,^5\Gamma$ state, the rest of the five quintets correlate adiabatically to a $4s^1 3d^6$ configuration of Mn (Fig. 4). In detail, the $b\,^5\Delta$, $c\,^5\Pi$, and $d\,^5\Sigma^+$ states correlate to the first excited state of Mn($a\,^6D;M_L=\pm2,\pm1,0$), respectively, 2.145 eV above the ground (^6S) state,[29] and theoretically at the MRCI (+Q) level 2.53 (1.97) eV. The $e\,^5\Phi$ and $g\,^5\Pi$ correlate to the $a\,^4F$ (or its almost degenerate

TABLE VIII. Results on MnF.[a]

Method	$-E$	r_e	D_e[b]	ω_e	$\omega_e x_e$	α_e	$\langle\mu\rangle/\mu_{\mathrm{FF}}$	q_{Mn}	T_e
				$X\,^7\Sigma^+$					
MRCI	1 249.804 51	1.856	107.8	611	2.9	0.0025	2.82/2.90	0.71	0.0
MRCI+Q	1 249.830 91	1.853	108.6	611	3.1	0.0026			0.0
MRACPF	1 249.829 31	1.855	107.0	607	2.7	0.0026	2.71/2.80	0.68	0.0
MRCI(+h)	1 249.805 32	1.856	107.8	611	3.0	0.0026	2.81	0.70	0.0
MRCI-DK	1 257.401 69	1.851	106.0	613	3.4	0.0027	2.78/2.90	0.82	0.0
MRCI-DK+Q	1 257.428 54	1.848	106.7	614	3.8	0.0027			0.0
C-MRCI	1 250.115 43	1.848	108.7	623	3.8	0.0026	2.82/2.90	0.72	0.0
C-MRCI+Q	1 250.178 99	1.843	110.9	623	3.4	0.0027			0.0
C-MRCI-DK	1 257.763 76	1.847	104.8	612	1.0	0.0031	2.82	0.83	0.0
C-MRCI-DK+Q	1 257.831 56	1.842	106.9	617	2.7	0.0028			0.0
RCCSD(T)	1 249.839 36	1.851	108.7	610	3.0	0.0027	/2.76		0.0
C-RCCSD(T)	1 250.199 77	1.840	110.2	609	3.5	0.0022	/2.75		0.0
Expt.[c]		1.8387	101.2±3.5[d] 104.5±2.3[d] 106.4±1.8[d]	624.2	3.2				
				$a\,^5\Sigma^+$					
MRCI	1 249.775 22	1.826	89.4	623	3.1	0.0026	2.76/3.20	0.65	6435
MRCI+Q	1 249.803 62	1.820	91.5	624	3.1	0.0025			5981
MRACPF	1 249.802 38	1.821	90.1	623	3.4	0.0026	2.78/3.25	0.63	5911
MRCI(+h)	1 249.776 16	1.826	89.5	623	3.1	0.0026	2.76/3.25	0.65	6401
MRCI-DK	1 257.371 91	1.817	87.3	624	2.8	0.0026	2.69	0.80	6540
MRCI-DK+Q	1 257.400 94	1.810	89.4	629	4.6	0.0026			6051
C-MRCI	1 250.084 18	1.817	89.0	634	3.1	0.0026	2.72/3.20	0.66	6855
C-MRCI+Q	1 250.149 80	1.808	92.5	639	3.6	0.0027			6401
C-MRCI-DK	1 257.731 71	1.812	84.6	632	7.7	0.0030	2.68	0.82	7030
C-MRCI-DK+Q	1 257.801 68	1.803	88.0	634	6.2	0.0025			6540
RCCSD(T)	1 249.808 77	1.809	89.5						6714
C-RCCSD(T)	1 250.161 88	1.772	86.5						8299
Expt.[c]		1.7854		645.92	3.22	0.0028			3000±1000
				$b\,^5\Delta$					
MRCI	1 249.685 73	1.756		668	4.0	0.0032	2.39/3.15	0.64	26057
MRCI+Q	1 249.718 05	1.744		680	4.0	0.0033			24763
MRACPF	1 249.716 94	1.743		677	4.3	0.0034	2.24	0.61	24658
C-MRCI	1 250.000 71	1.753		685		0.0018	2.41	0.66	25182
C-MRCI+Q	1 250.072 09	1.739		689	7.8	0.0031			23469
				$c\,^5\Pi$					
MRCI	1 249.683 83	1.786	90.5	666	4.9	0.0031	2.74/3.71	0.65	26476
MRCI+Q	1 249.715 43	1.777	91.4	672	3.5	0.0029			25357
C-MRCI	1 249.999 48	1.782	91.4	674	6.8	0.0028	2.70	0.67	25462
C-MRCI+Q	1 250.070 23	1.770	93.5	684	6.4	0.0032			23853
Expt.[c]		1.788		630.54	3.564	0.0024			11751
				$d\,^5\Sigma^+$					
MRCI	1 249.675 37	1.807		630	2.8	0.0026	2.58/3.05	0.67	28330
MRCI+Q	1 249.707 71	1.793		639	2.9	0.0027			27036
MRACPF	1 249.707 00	1.790		634	3.0	0.0027	2.38	0.64	26861
C-MRCI	1 249.990 35	1.804		640	6.5	0.0026	2.62	0.68	27456
C-MRCI+Q	1 250.061 42	1.788		651	6.8	0.0026			25812
Expt.[c]		1.8193		597.38	3.15	0.0031			14493
				$A\,^7\Pi$					
MRCI	1 249.675 72	1.819	71.1	633	3.2	0.0028	4.18/4.22	0.65	28576[e]
MRCI+Q	1 249.702 72	1.814	76.1	631	1.8	0.0025			28364
C-MRCI	1 249.985 53	1.808	69.7				4.18	0.67	29052[e]
C-MRCI+Q	1 250.049 38	1.801	76.3						28974
RCCSD(T)	1 249.709 59	1.813	73.3	636	3.2	0.0027	/4.08		28481
C-RCCSD(T)	1 250.068 31	1.799	79.3	650	3.2	0.0025	/3.93		28851
Expt.[c]		1.7923		648.0	1.6	0.0029			28526
				$e\,^5\Phi$					
MRCI	1 249.673 44	1.821	138.0	647	0.7	0.0012	2.43/2.44	0.68	28750
MRCI+Q	1 249.703 43	1.814	137.6	651	3.5	0.0020			27980
C-MRCI	1 249.989 78	1.814	136.4	645			2.47	0.70	27596
C-MRCI+Q	1 250.058 81	1.805	136.2	653					26372
				$f\,^5\Gamma$					
MRCI	1 249.669 27	1.841		619	2.5	0.0026	2.55/2.59	0.69	29694
MRCI+Q	1 249.698 74	1.836		623	2.9	0.0026			28995
C-MRCI	1 249.985 81	1.832		634	6.7	0.0026	2.56	0.70	28435
C-MRCI+Q	1 249.054 31	1.825		638	6.9	0.0027			27351
				$g\,^5\Pi$					
MRCI	1 249.668 26	1.813	98.1	653	5.5	0.0027	2.40/2.36	0.67	29904
MRCI+Q	1 249.700 77	1.805	98.6	649	5.0	0.0029			28575
C-MRCI	1 249.983 42	1.805	100.0	654	6.3	0.0025	2.46	0.69	28960
C-MRCI+Q	1 250.055 63	1.796	102.0	658	5.8	0.0024			27071
Expt.[c]		1.8101		640	3.6				19807
				$h\,^5\Pi$					
MRCI	1 249.647 80	1.998	122.2	763			4.84/4.63	0.77	34381
C-MRCI	1 249.959 97	2.002	118.2	780			5.24	0.78	34136
C-MRCI+Q	1 250.044 31	1.985	127.7	782					29554
				$i\,^5\Pi$					
MRCI	1 249.634 83	1.852		631	3.8	0.0021	2.69/2.75	0.69	37249
MRCI+Q	1 249.666 75	1.838		609	3.3	0.0018			36025
C-MRCI	1 249.951 51	1.848		623			2.75	0.70	35990
C-MRCI+Q	1 250.023 38	1.834		618	7	0.0031			34136

[a]Symbols, units, and acronyms as in Table IV.
[b]With respect to adiabatic fragments.
[c]See Table I.
[d]D_0.
[e]The MRCI (C-MRCI) energy of the $X\,^7\Sigma^+$ state using the extended CASSCF space is $-1\,249.805\,92$ ($-1\,250.117\,90$) hartree.

companion $a\,^4H$) and $a\,^4D$ atomic states of Mn, 2.20 and 0.61 eV above the $a\,^5D$ state,[29] respectively. At the MRCI (+Q) levels these gaps are 2.34 (2.33) and 0.75 (0.71) eV. Finally, the $f\,^5\Gamma$ state traces its origin to the $a\,^4G(4s^2 3d^5)$ state of the metal, 0.99 eV higher than the $a\,^6D$. For technical reasons we were not able to construct PECs of the $b\,^5\Delta$, $d\,^5\Sigma^+$, and $f\,^5\Gamma$ states beyond 3 Å of interatomic distance (Fig. 4).

Following the M^+F^- model, and according to our Mulliken populations around equilibrium, the *in situ* Mn^+ atom and in all six quintet states is described by a $4s^1 3d^5$ configuration. It seems, that the only Mn^+ spectroscopic terms consistent with the $4s^1 3d^5$ distribution and spin–orbital angular momentum, are of $a\,^5G$ and $a\,^5P$ symmetries, 3.42 and 3.71 eV above the $a\,^7S$ Mn^+ state.[29]

Experimentally, certain results are available for the $c\,^5\Pi$, $d\,^5\Sigma^+$, and $g\,^5\Pi$ states, tagged (from the experimentalists) as $b\,^5\Pi_i$,[21] $c\,^5\Sigma^+$ or $e\,^5\Sigma^+$,[18,20] and $d\,^5\Pi$,[19,20] respectively (see also Table I). These states are most easily accessible from the first excited $a\,^5\Sigma^+$ state of MnF, and indeed, all experimentally reported T_e energies are with respect to the $a\,^5\Sigma^+$ state. Moving directly to the $c\,^5\Pi$ state, at the C-MRCI+Q level we obtain $T_e(c\,^5\Pi \leftarrow X\,^7\Sigma^+) = 23853\,\mathrm{cm}^{-1}$ at $r_e = 1.770$ Å (1.7883 Å experimentally[21]). The T_e value should be reduced by 6401 cm^{-1}, the $a\,^5\Sigma^+ - X\,^7\Sigma^+$ separation energy at the same level (*vide supra*), in order to be compared with the experimental results. Therefore, we obtain $T_e = 23853 - 6401 = 17452\,\mathrm{cm}^{-1}$, larger by 5701 cm^{-1} from the experimental value. Assuming that the experimental number is reliable and that *we are referring to the same state*, this ~5500 cm^{-1} discrepancy could be attributed to our inability to cope with such complex systems. However, and along these lines, it should be mentioned that according to the experimentalists[21] the *in situ* Mn^+ in the $c\,^5\Pi$ ($b\,^5\Pi_i$ for them) state, is an $a\,^5D(3d^6)$ state, 1.81 eV above the $a\,^7S$ state. On the other hand, our calculations indicate rather clearly as was already mentioned, that the equilibrium Mn^+ ion finds itself in the $a\,^5G(4s^1 3d^5)$ term, 0.99 eV (=7985 cm^{-1}) *higher* than the $a\,^5D(3d^6)$ term. It is not unlikely that, calculationally, as the two atoms approach from infinity $[\mathrm{Mn}(4s^1 3d^6) + \mathrm{F}(^2P)]$ and well after the "ionic avoided crossing" around 3 Å where we have $Mn^+(3d^6) + F^-(^1S)$, our calculations "lock" in the $a\,^5G(4s^1 3d^5)$ state of Mn^+ ($r = 2.15$ Å), they lose their variational character and follow this path until equilibrium. Therefore we are rather referring to a different $^5\Pi$ state. That perhaps we have calculated a higher $^5\Pi$ state is also supported by the fact that even at the MRCI level our r_e is smaller, and ω_e larger than the experimental ones. At the C-MRCI+Q level these differences magnify to $\Delta r_e = -0.018$ Å and $\Delta\omega_e = +53.5\,\mathrm{cm}^{-1}$, a rather unusual behavior for MRCI calculations and taking into account all our previous results on the MF systems. Certainly, further investigation is needed to clarify this point.

For the $d\,^5\Sigma^+$ state the C-MRCI+Q $T_e(d\,^5\Sigma^+ \leftarrow X\,^7\Sigma^+)$ is 25812 cm^{-1}. As before, this value should be reduced by 6401 cm^{-1} in order to obtain the energy separation with respect to the $a\,^5\Sigma^+$ state, $T_e(d\,^5\Sigma^+ \leftarrow a\,^5\Sigma^+) = 19411\,\mathrm{cm}^{-1}$. This value is 4918 cm^{-1} larger than the experimental one named $c\,^5\Sigma^+$.[18] As in the previously discussed $^5\Pi$ state, the same comments apply here concerning the r_e and ω_e values (Table VIII). However, in Table I, experimental Ref. 20, an $e\,^5\Sigma^+$ state is given with a $T_e(e\,^5\Sigma^+ \leftarrow a\,^5\Sigma^+) = 20220\,\mathrm{cm}^{-1}$, and a similar configurational electron distribution as in Eq. (29); no other experimental information or comments are presented. This latter T_e value can be considered in fair agreement with our $d\,^5\Sigma^+ - a\,^5\Sigma^+$ separation, the difference being 809 cm^{-1}.

For the $g\,^5\Pi$ state ($d\,^5\Pi$ according to Ref. 19), at the C-MRCI+Q level we calculate an energy gap $T_e(g\,^5\Pi \leftarrow a\,^5\Sigma^+) = 27071 - 6401 = 20670\,\mathrm{cm}^{-1}$, 863 cm^{-1} larger than the experimental one.[19] At the same level of theory, C-MRCI (+Q), we obtain $r_e = 1.805(1.796)$ Å and $\omega_e = 654(658)\,\mathrm{cm}^{-1}$ in good agreement with the experimental findings. As was discussed in the introduction of the present subsection, the electron distribution of the *in situ* Mn^+ ion is $4s^1 3d^5$ arising from the $a\,^5G$ or $a\,^5P$ terms of Mn^+ differing by 0.29 eV (Ref. 29) [see also Eq. (33)]. However, this is not the interpretation given by Launila and Simard:[19] It is claimed, with some reservation, that the *in situ* Mn^+ term finds itself in a $4p^1 3d^5$ configuration; the lowest Mn^+ term corresponding to such a distribution is $z\,^5P^0[3d^5(a\,^6S)4p^1]$, 5.39 eV above the ground Mn^+ state.[29] Obviously, we do not agree with this interpretation.

3. $A^7\Pi$

This is an interesting high-spin state directly accessible from the $X\,^7\Sigma^+$ state. Within our M^+F^- equilibrium model the lowest Mn^+ term conforming to a Π angular momentum symmetry is $z\,^7P^0(3d^5 4p^1)$, 4.503 eV above the $a\,^7S$ ground state.[29] Certainly, its proper description requires a full set of $4p$ Mn orbitals to be included in the CASSCF active space (see Sec. II). The result of increasing the reference space by two orbital functions, leads to a dramatic increase of the icMRCI configurational size to about 4.2×10^6 configurations; the corresponding C-MRCI expansion contains $\sim 20\times10^6$ configurations rendering the calculations, indeed, painful.

The CASSCF equilibrium configurations and Mulliken atomic distributions are

$$|A\,^7\Pi\rangle_{B_1} = 0.994|3\sigma^1 2\pi_x^1 3\pi_x^1 2\pi_y^1 1\delta_+^1 1\delta_-^1\rangle, \qquad (34)$$

where, $3\sigma = 0.97(3d\sigma)$, $2\pi_x = 3\mathrm{d}\pi_x$, $3\pi_x = 4p_x$, $2\pi_y = 3\mathrm{d}\pi_y$, $1\delta_+ = 3\mathrm{d}_{\delta+}$, $1\delta_- = 3\mathrm{d}_{\delta-}$; $4s^{0.14}4p_z^{0.04}3d_{z^2}^{1.01}\ 3d_{xz}^{1.05}\ 3d_{yz}^{1.01}3d_{x^2-y^2}^{1.00}3d_{xy}^{1.00}4p_x^{1.01}/2s^{1.99}2p_z^{1.81}2p_x^{1.92}2p_y^{1.96}$. The bonding is succinctly described by the following vbL icon

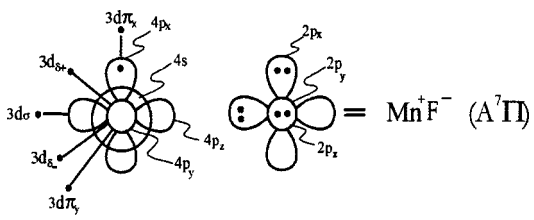

$Mn^+(^7P; M_L = \pm 1)$ $F^-(^1S)$

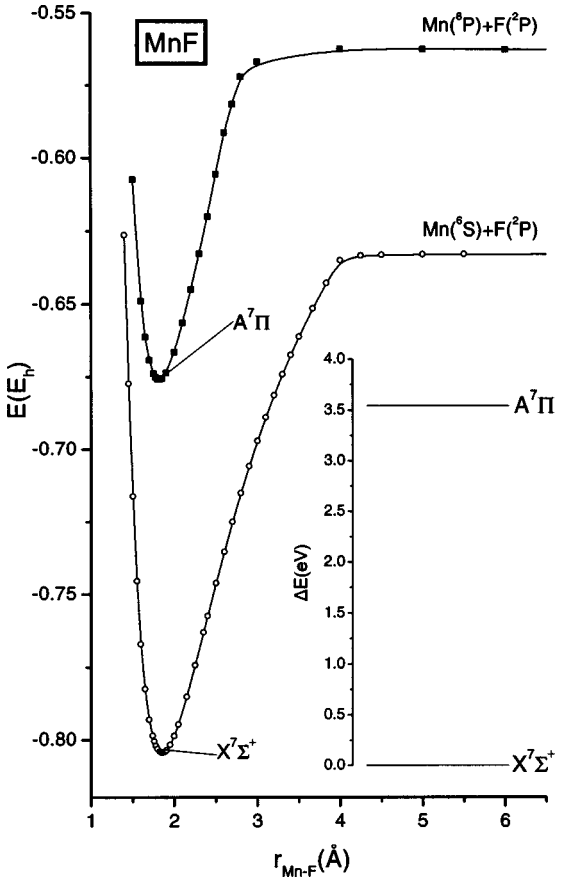

FIG. 5. $X\,^7\Sigma^+$ and $A\,^7\Pi$ MRCI potential energy curves of MnF and a two level diagram inset.

Adiabatically, the $A\,^7\Pi$ state correlates to $\mathrm{Mn}(z\,^8P^0;3d^5 4s^1 4p^1)+\mathrm{F}(^2P)$, 2.303 eV above the $a\,^6S$ state,[29] calculated 1.912 (2.08) eV at the MRCI (+Q) level. Figure 5 shows the MRCI $A\,^7\Pi$ potential energy curve along the $X\,^7\Sigma^+$ curve for reasons of clarity.

Experimentally, $T_e(A\,^7\Pi \leftarrow X\,^7\Sigma^+)=28526\,\mathrm{cm}^{-1}$ and $r_e=1.7923$ Å.[20] At the MRCI (+Q) level we calculate $T_e(A\,^7\Pi \leftarrow X\,^7\Sigma^+)=28576(28364)$ in remarkable, and rather coincidental agreement due to cancellation of errors, with the experimental value. As usual, the MRCI (+Q) bond length is larger than the experimentally determined value by 0.027 (0.022) Å. Inclusion of core-correlation effects shortens the bond length by 0.011 (0.013) Å at the C-MRCI (C-MRCI+Q) level, bringing the agreement between theory and experiment within 0.016 (0.009) Å. However, at this level of approximation the $A\,^7\Pi - X\,^7\Sigma^+$ splitting becomes slightly worse, $T_e=29052(28974)\,\mathrm{cm}^{-1}$ (Table VIII). The absolute single reference character of both $X\,^7\Sigma^+$ and $A\,^7\Pi$ states, renders their description by the coupled-cluster approach particularly informing. RCCSD(T) [C-RCCSD(T)] T_e and r_e values are 28481 [28851] cm^{-1}, 1.813 [1.799] Å, in excellent agreement with experimental values. Notice that the r_e and ω_e of the $A\,^7\Pi$ state are significantly shorter and larger, respectively, from the corresponding values of the $X\,^7\Sigma^+$ state, while the latter's D_e value is by 37 kcal/mol (MRCI) larger as compared to the $A\,^7\Pi$ state. These seemingly contradicting results fall into the right perspective if we consider the intrinsic bond strengths of $A\,^7\Pi$ and $X\,^7\Sigma^+$, i.e., their dissociation energies not with respect to adiabatic fragments $\mathrm{Mn}(z\,^8P^0)+\mathrm{F}(^2P)$, $\mathrm{Mn}(a\,^6S)+\mathrm{F}(^2P)$, but with respect to the diabatic ions $\mathrm{Mn}^+(z\,^7P^0)+\mathrm{F}^-(^1S)$, $\mathrm{Mn}^+(a\,^7S)+\mathrm{F}^-(^1S)$. For the $A\,^7\Pi$ we write, $D_e(A\,^7\Pi,\mathrm{diabatic}) = D_e(\mathrm{adiabatic})+\mathrm{IP(Mn)}-\mathrm{EA(F)}-\Delta E[z\,^8P^0(\mathrm{Mn}) \leftarrow a\,^6S(\mathrm{Mn})]+\Delta E[z\,^7P^0(\mathrm{Mn}^+) \leftarrow a\,^7S(\mathrm{Mn}^+)]$. Using the MRCI +Q [C-RCCSD(T)] values we obtain (Tables III, VIII) $D_e(A\,^7\Pi,\ \mathrm{diabatic}) = 76.1[79.3]\,\mathrm{kcal/mol} + 7.248[7.317]\,\mathrm{eV} - 3.24[3.38]\,\mathrm{eV} - 2.08[2.24]\,\mathrm{eV} + 4.54[4.66]\,\mathrm{eV} = 225.3[225.9]\,\mathrm{kcal/mol}$. In analogy, for the $X\,^7\Sigma^+$ state we have $D_e(X\,^7\Sigma^+,\mathrm{diabatic}) = 108.6[110.2]\,\mathrm{kcal/mol} + 7.248[7.317]\ \mathrm{eV} - 3.24[3.38]\ \mathrm{eV} = 201.0[201.0]\ \mathrm{kcal/mol}$. Therefore the $D_e(A\,^7\Pi,\mathrm{diabatic})$ is larger than the $D_e(X\,^7\Sigma^+,\mathrm{diabatic})$ by about 13%, thus making the r_e and ω_e differences between the two states previously discussed more reasonable.

4. $h^5\Pi$, $i^5\Pi$

The $h\,^5\Pi$ state correlates adiabatically to $\mathrm{Mn}(3d^6 4s^1;b\,^4P^0)$ (Ref. 29) $+\mathrm{F}(^2P)$, but for technical reasons we were not able to construct the repulsive part of the potential energy curve, Fig. 4. The $i\,^5\Pi$ state, 2868 cm^{-1} above the $h\,^5\Pi$ state at the MRCI level, seems to correlate to a $a\,^4H(3d^6 4s^1)$ (Ref. 29) state of Mn, but we are missing the PEC's part from 4 Å and beyond (Fig. 4). The leading CASSCF equilibrium configurations are

$$|h\,^5\Pi\rangle_{B_1} \approx |[(0.88)4\sigma^1+(0.27)3\sigma^1]2\pi_x^2 2\pi_y^1 1\delta_+^1 1\delta_-^1\rangle, \tag{35}$$

$$|i\,^5\Pi\rangle_{B_1} \approx |4\sigma^1[(0.55)3\sigma^1 1\delta_+^2+(0.37)3\sigma^2 1\delta_+^1]2\pi_y^1 1\delta_-^1\rangle + |(0.48)3\sigma^1[4\sigma^1 2\pi_x^1 2\pi_y^2+2\pi_x^2 2\pi_y^1 1\delta_-^1]1\delta_+^1\rangle, \tag{36}$$

with, about 0.8 and 0.7 e^- transferred from Mn to F atom, in the h and $i\,^5\Pi$ states, and *in situ* populations pertaining to $3d^6(a\,^5D)$ and $4s^1 3d^5$ of Mn^+, respectively. Numerical results for these states are given in the last two entries of Table VIII, but we have to admit that our values are only indicative due to many technical difficulties.

E. Dipole moments

For reasons of easy comparison dipole moments of the four MF (M=Ti,V,Cr,Mn) X-states calculated in different methods are collected in Table IX. A first observation within the $\mathrm{M}^+\mathrm{F}^-$ binding model, is, that dipole moment magnitudes do not conform to a classical (point) charge distribution scheme. For instance, for the TiF $X\,^4\Phi$ state $\mu_{\mathrm{FF}}(\mathrm{C\text{-}MRCI}) = 2.95\,\mathrm{D}$; using Mulliken charges we calculate classically, $\mu_{\mathrm{C}} = q_{\mathrm{Ti}} \times r_e = 0.74 \times 3.49\,\mathrm{a.u.} = 6.6\,\mathrm{D}$. The discrepancy is much larger for the $c\,^2\Sigma^-$ of TiF where $\mu_{\mathrm{FF}}(\mathrm{MRCI}) = 1.78\,\mathrm{D}$ (Table IV) vs $\mu_{\mathrm{C}} = 6.2\,\mathrm{D}$. Although Mulliken charges are not very reliable, one needs effective charges of 0.3 or 0.2 e^- to obtain $\mu_{\mathrm{FF}} \approx \mu_{\mathrm{C}}$ for these two states, and certainly this is not the case for the MF systems. The problem can be rather traced to the fact that we are dealing not

TABLE IX. Dipole moments $\langle\mu\rangle/\mu_{FF}$[a] (Debye) of the ground state fluorides in different methodologies.

Method[b]	TiF($X\,^4\Phi$)	VF($X\,^5\Pi$)	CrF($X\,^6\Sigma^+$)	MnF($X\,^7\Sigma^+$)
MRCI	2.54/2.85	2.31/2.77	4.43/4.27	2.82/2.90
C-MRCI	2.48/2.95	2.27/2.82	4.48/4.27	2.82/2.90
MRCI-DK	2.51/2.81	2.28/2.72	3.04/3.56	2.78/2.90
C-MRCI-DK	2.47	2.27	3.06	2.82
RCCSD(T)	/2.95	/3.05	/4.35	/2.76
C-RCCSD(T)	/2.80	/3.25	/4.22	/2.75
MRCI/A5Z[c]	2.49/2.80			
C-MRCI/A5Z[d]	2.42/2.85			

[a]$\langle\mu\rangle$ calculated as an expectation value, μ_{FF} obtained by the finite field method.
[b]Acronyms as in Table IV.
[c]Using the quintuple correlation consistent-like basis of Ti and the aug-cc-pV5Z of F: $[7s8p6d4f3g2h1i/_{Ti}7s6p5d4f3g2h/_{F}]$.
[d]As in c but augmented by a series of $[1f1g1h]$ core functions for Ti, see text.

only with highly ionic, but also highly open systems, with very complex spatial electron distributions which cannot be ''simulated'' by two opposite point charges.

The same observations hold true for the dipole moments of the entire MF series and all states presently studied. Figure 6 shows the dependence of μ $(=\langle\mu\rangle)$ as a function of interatomic distance of the four X-states. As it should, $\mu\approx 0$ from infinity to $r_{M-F}\approx 4-4.5$ Å where the ionic avoided crossing takes over and a whole electron is transferred from M to F. At this point μ jumps to, for instance, 18.6 D for TiF($X\,^4\Phi$), close to its ''classical'' value $\mu_C = r\times q = (4.5/0.53)\times 1\times 2.54 = 21.6$ D, and the same is practically true for VF, CrF, and MnF X-states. Approaching r_e, μ reduces almost linearly to its final equilibrium value, on the average smaller than the corresponding μ_C by about 3 D. This ''dipole moment loss'' reflects the complex distribution of the open spectator electrons and polarization effects upon interaction.

A second observation concerns expectation value $\langle\mu\rangle$ vs finite field μ_{FF} dipole moments. From Table IX it is clear that, with the exception of CrF (but see below), μ_{FF} is larger than $\langle\mu\rangle$. It is our belief that μ_{FF} values are in general more reliable than $\langle\mu\rangle$ values for reasons rationalized in Ref. 43.

A comment is needed for the dipole moment of the X-state of CrF. Table IX shows that MRCI $\langle\mu\rangle$ or μ_{FF} values of TiF, VF, and MnF do not change by more than 0.05 D at the MRCI-DK level. The same is expected at the C-MRCI versus C-MRCI-DK level. An exception is noted in the $X\,^6\Sigma^+$ state of CrF: The addition of DK-relativistic corrections reduces its MRCI $\langle\mu\rangle/\mu_{FF} = 4.43/4.27$ to 3.04/3.56 D, a change of 1.4/0.7 D. We confess that the decrease of $\langle\mu\rangle$ by 1.4 D is at least suspicious. The μ_{FF} MRCI-DK value is more reasonable but still 0.7 D smaller than the MRCI μ_{FF} result. Harrison reports $\langle\mu\rangle = 4.16$ and 4.23 D at the MRCI and C-MRCI levels, respectively, for the $X\,^6\Sigma^+$ state of CrF.[27] As a final comment, and taking also into account the RCCSD(T) μ_{FF} values, we can say that the dipole moment of the X-states of TiF, VF, and MnF is very close to 3 D, while our best estimate for the X-state of CrF is close to 4 D.

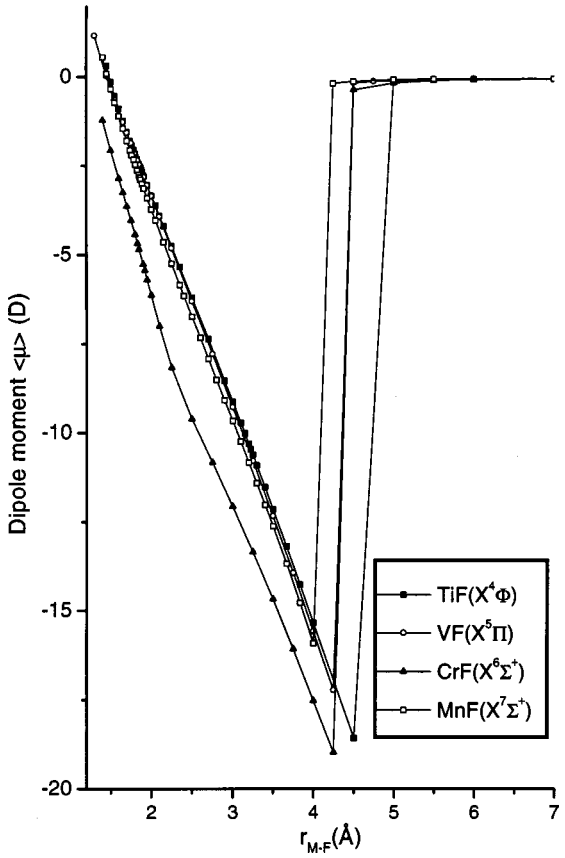

FIG. 6. MRCI dipole moments $\langle\mu\rangle$ of the TiF, VF, CrF, and MnF ground states as a function of interatomic distance.

V. SUMMARY AND CONCLUDING REMARKS

Using multireference (CASSCF+1+2) and coupled cluster [RCCSD(T)] methods in conjunction with large to very large basis sets (TiF), we have investigated the electronic structure of the diatomic fluorides TiF, VF, CrF, and MnF. We report total energies, dissociation energies, spectroscopic constants $(r_e, \omega_e, \omega_e x_e, \alpha_e)$, dipole moments, Mulliken distributions, and potential energy curves (PEC) for a total of 34 states. Relativistic effects through the Douglas–Kroll approximation were also examined for the ground and first excited states. Our most important findings can be synopsized as follows:

(1) The ground states of TiF, VF, CrF, and MnF are of $^4\Phi$, $^5\Pi$, $^6\Sigma^+$, and $^7\Sigma^+$ symmetries, respectively. Note, that it is the first time that the X-states of TiF and VF have been established with certainty, with their first excited states $A\,^4\Sigma^-$, $A\,^5\Delta$ located about 2 and 3 kcal/mol higher.
(2) Taking into account the totality of our numerical findings as well as the existing experimental results, our best ''estimated'' D_e values with respect to ground state neutral atoms for the X-states, are, 135, 130, 110, and 108 kcal/mol for TiF, VF, CrF, and MnF, respectively. Note that no experimental or theoretical D_e results on the VF have been reported before.
(3) In all four MF molecules and states and in harmony with chemical empiricism, the *in situ* atoms indicate a promi-

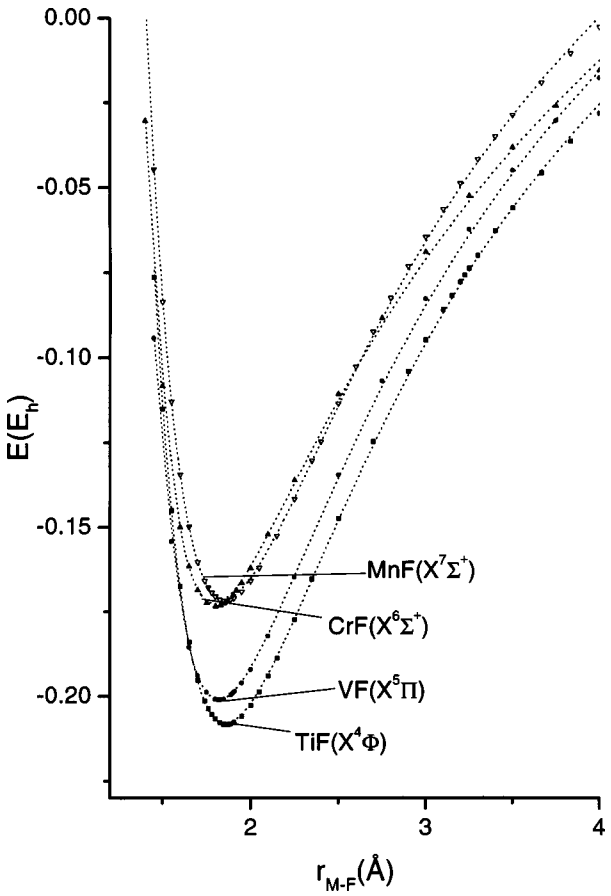

FIG. 7. Fitted potential curves (dotted lines) of the TiF, VF, CrF, and MnF ground state MRCI calculated curves to a Rittner-type potential. See text.

nent ionic character (about $0.7-0.8\,e^-$ are transferred from M to F), as inferred from the Mulliken population analysis. To corroborate further this result we fitted our ground state PECs to a Rittner-type formula[50]

$$V(r)=-\frac{1}{r}-\frac{A}{r^4}+Be^{-r/C},$$

where, *A*, *B*, and *C* are freely adjustable parameters. It is reminded that the Rittner formula has been derived from purely classical arguments to account for the dissociation energies of the ionic alkali halides (MeX,Me=Na,K,...,X=F,Cl,...) in the gas phase.[50] The results shown in Fig. 7 are in perfect agreement with the MRCI PECs up to $r=4$ Å, indicating nicely the dominance of the $-1/r$ Coulombic term. We remind that the ionic avoided crossings occur at about 4 Å of interatomic distance. The *A*, *B*, *C* fitting parameters, useful because they describe almost perfectly our calculated points, are

$\mathrm{TiF}(X\,^4\Phi)$: $-3.510,\ -6.441,\ 0.518,$

$\mathrm{VF}(X\,^5\Pi)$: $-3.426,\ -8.008,\ 0.485,$

$\mathrm{CrF}(X\,^6\Sigma^+)$: $-4.509,\ -21.327,\ 0.411,$

$\mathrm{MnF}(X\,^7\Sigma^+)$: $-3.682,\ -9.085,\ 0.474.$

An observation is in order here. In the original Rittner potential[50] $A=(\alpha_1+\alpha_2)/2$, where α_1, α_2 are the polarizabilities of the two interacting atoms $(\mathrm{Me}^+,\mathrm{X}^-)$. Therefore, the $-A/r^4$ term is *negative* resulting to an increase of the binding energy due to the leading $-1/r$ Coulombic interaction as it should. In the present case however the $-A/r^4$ is *positive* (*A* negative), certainly due to the fact that the (absolute) total charge distribution on M and F is less than 1 after the ionic crossing, thus diminishing the overestimated Coulombic interaction.

(4) The contribution of Douglas–Kroll relativistic effects is not significant, practically for all calculated properties in this series of molecular systems. More importantly, in the case of $\mathrm{TiF}(X\,^4\Phi, A\,^4\Sigma^-)$, it was found that by increasing significantly the basis set size, therefore increasing the extracted correlation energy, DK-effects practically vanish.

(5) The overwhelming ionic character of these molecules is reflected in the striking similarities of certain properties. For instance for the *X*-states, C-MRCI harmonic frequencies do not differ by more than 30 cm^{-1} from an average value of 650 cm^{-1} along the MF series. The same can be said for the interatomic distances; small differences observed moving from TiF to MnF (C-MRCI), no more than 0.03 Å from an average value of 1.824 Å, reflect small differences in the ionic radii of the *in situ* M^+ atoms.

(6) Finally, it can be said that plain MRCI results give a fair overall description of the MF molecules, but core-correlation effects (C-MRCI) are necessary to bring bond distances in harmony with experimental results, and that the coupled-cluster approach, particularly when core effects are included [C-RCCSD(T)], gives excellent results for single reference states.

Note added in proof. In an experimental paper of TiF published by P. M. Sheridan, S. K. McLamarrah, and L. M. Ziurys, J. Chem. Phys. **119**, 9496 (2003), it is definitely established that the ground state symmetry of TiF is $^4\Phi_r$.

ACKNOWLEDGMENTS

C.K. and S.K. express their gratitude to the Hellenic State Scholarship Foundation (IKY) for financial support. The computing time provided by the National Center for Scientific Research, DEMOKRITOS, is greatly appreciated.

[1] J. F. Harrison, Chem. Rev. **100**, 679 (2000) and references therein.
[2] R. S. Ram, J. R. D. Peers, Y. Teng, A. G. Adam, A. Muntianu, P. F. Bernath, and S. P. Davis, J. Mol. Spectrosc. **184**, 186 (1997).
[3] A. J. Cernicharo and M. Guélin, Astron. Astrophys. **183**, L10 (1987); L. M. Ziurys, A. J. Apponi, and T. G. Phillips, Astrophys. J. **433**, 729 (1994).
[4] K. F. Zmbov and J. L. Margrave, J. Chem. Phys. **47**, 3122 (1967).
[5] K. F. Zmbov and J. L. Margrave, J. Phys. Chem. **71**, 2893 (1967).
[6] R. A. Kent and J. L. Margrave, J. Am. Chem. Soc. **86**, 5090 (1965).
[7] R. A. Kent, T. C. Ehlert, and J. L. Margrave, J. Am. Chem. Soc. **86**, 5090 (1964).
[8] R. L. Diebner and J. G. Kay, J. Chem. Phys. **51**, 3547 (1969).
[9] E. A. Shenyavaskaya and V. M. Dubov, J. Mol. Spectrosc. **113**, 85 (1985).
[10] W. E. Jones and G. Krishnamurty, J. Phys. B **13**, 3375 (1980).
[11] R. S. Ram, P. F. Bernath, and S. P. Davis, J. Chem. Phys. **116**, 7035 (2002).
[12] O. V. Boltalina, A. Y. Borshchevskii, and L. N. Sidorov, Russ. J. Phys. Chem. **65**, 466 (1991).

[13] O. Launila, J. Mol. Spectrosc. **169**, 373 (1995).
[14] R. Koivisto, S. Wallin, and O. Launila, J. Mol. Spectrosc. **172**, 464 (1995).
[15] S. Wallin, R. Koivisto, and O. Launila, J. Chem. Phys. **105**, 388 (1996).
[16] T. Okabayashi and M. Tanimoto, J. Chem. Phys. **105**, 7421 (1996).
[17] R. Koivisto, O. Launila, B. Schimmelpfennig, B. Simard, and U. Wahlgren, J. Chem. Phys. **114**, 8855 (2002).
[18] O. Launila and B. Simard, J. Mol. Spectrosc. **154**, 93 (1992).
[19] O. Launila and B. Simard, J. Mol. Spectrosc. **154**, 407 (1992).
[20] O. Launila, B. Simard, and A. M. James, J. Mol. Spectrosc. **159**, 161 (1993).
[21] B. Simard and O. Launila, J. Mol. Spectrosc. **168**, 567 (1994).
[22] T. C. Devore and J. L. Gole, J. Phys. Chem. **100**, 5660 (1996).
[23] G. Balducci, M. Campodonico, G. Gigli, G. Meloni, and S. N. Cesaro, J. Chem. Phys. **117**, 10613 (2002).
[24] A. I. Dement'ev and V. Ya. Simkin, Russ. J. Phys. Chem. **61**, 1408 (1987).
[25] A. I. Boldyrev and J. Simons, J. Mol. Spectrosc. **188**, 938 (1998).
[26] A. S. Averyanov and Yu. G. Khait, Opt. Spektrosk. **67**, 827 (1990).
[27] J. F. Harrison, Mol. Phys. **97**, 1009 (1999).
[28] J. F. Harrison, J. Phys. Chem. **87**, 1312 (1983).
[29] C. A. Moore, Atomic Energy Levels, NRSDS-NBS, Circ. No. 35 (U.S. GPO, Washington, D.C., 1971).
[30] T. H. Dunning, Jr., J. Chem. Phys. **90**, 1007 (1989); R. A. Kendall, T. H. Dunning, Jr., and R. J. Harrison, *ibid.* **96**, 6796 (1992).
[31] C. W. Bauschlicher, Jr., Theor. Chim. Acta **92**, 183 (1995).
[32] C. W. Bauschlicher, Jr., Theor. Chem. Acc. **103**, 141 (1999).
[33] H.-J. Werner and P.-J. Knowles, J. Chem. Phys. **89**, 5803 (1988); P. J. Knowles, H.-J. Werner, and E. A. Reinsch, *ibid.* **76**, 3144 (1982); H.-J. Werner, Adv. Chem. Phys. **LXIX**, 1 (1987).
[34] MOLPRO 2000 is a package of *ab initio* programs designed by H.-J. Werner and P. J. Knowles, version 2002.6, R. D. Amos, A. Bernhardsson, A. Berning *et al.*
[35] K. A. Peterson, D. E. Woon, and T. H. Dunning, Jr., J. Chem. Phys. **100**, 7410 (1994).
[36] M. Douglas and N. M. Kroll, Ann. Phys. (N.Y.) **82**, 89 (1974).
[37] B. A. Hess, Phys. Rev. A **32**, 756 (1985); **33**, 3742 (1986).
[38] R. J. Gdanitz and R. Ahlrichs, Chem. Phys. Lett. **143**, 413 (1988); H.-J. Werner and P. J. Knowles, Theor. Chim. Acta **84**, 95 (1992).
[39] H. B. Jansen and P. Ross, Chem. Phys. Lett. **3**, 140 (1969); S. F. Boys and F. Bernardi, Mol. Phys. **19**, 553 (1970).
[40] E. V. R. de Castro and F. E. Jorge, J. Chem. Phys. **108**, 5225 (1998); C. F. Bunge, J. A. Barrientos, A. V. Bunge, and J. A. Cogordan, Phys. Rev. A **46**, 3691 (1992).
[41] ACES II is a program product of the Quantum Theory Project, University of Florida, J. F. Stanton, J. Gauss, J. D. Watts *et al.*, Integral packages included are VMOL, J. Almlöf and P. R. Taylor; VPROPS, P. Taylor; ABACUS, T. Helgaker, H. J. Aa. Jensen, P. Jørgensen, J. Olsen, and P. R. Taylor.
[42] C. Blondel, Phys. Scr. **58**, 31 (1995).
[43] D. Tzeli and A. Mavridis, J. Chem. Phys. **118**, 4984 (2003).
[44] A. J. Merer, Annu. Rev. Phys. Chem. **40**, 407 (1989).
[45] R. S. Ram, P. F. Bernath, and S. P. Davis, J. Chem. Phys. **114**, 4457 (2001).
[46] F. A. Jenkins, Joint Commission for Spectroscopy **43**, 425 (1953).
[47] P. M. Sheridan and L. M. Ziurys, Chem. Phys. Lett. **380**, 632 (2003).
[48] G. D. Rochester and E. Olsson, Z. Phys. **114**, 495 (1939).
[49] T. C. DeVore, R. J. Van Zee, and W. Weltner, Jr., J. Chem. Phys. **68**, 3522 (1978).
[50] E. S. Rittner, J. Chem. Phys. **19**, 1030 (1951).